

Quantum Self-Propulsion of an Inhomogeneous Object out of Thermal Equilibrium

Kimball A. Milton,^{1,*} Nima Pourtolami,^{2,†} and Gerard Kennedy^{3,‡}

¹*H. L. Dodge Department of Physics and Astronomy,
University of Oklahoma, Norman, OK 73019, USA*

²*National Bank of Canada, Montreal, Quebec H3B 4S9, Canada*

³*School of Mathematical Sciences, University of Southampton, Southampton, SO17 1BJ, UK*

(Dated: May 27, 2024)

In an earlier paper, we explored how quantum vacuum torque can arise: a body or nanoparticle that is out of thermal equilibrium with its environment experiences a spontaneous torque. But this requires that the body be composed of nonreciprocal material, which seems to necessitate the presence of an external influence, such as a magnetic field. Then the electric polarizability of the particle has a real part that is nonsymmetric. This effect occurs to first order in the polarizability. To that order, no self-propulsive force can arise. Here, we consider second-order effects, and show that spontaneous forces can arise in vacuum, without requiring exotic electromagnetic properties. Thermal nonequilibrium is still necessary, but the electric susceptibility of the body need only be inhomogeneous. We investigate four examples of such a body: a needle composed of distinct halves; a sphere and a ball, each hemisphere being made of a different substance; and a thin slab, each face of which is different. The results found are consistent with previous numerical investigations. Here, we take into account the skin depth of metal surfaces. We also consider the frictional forces that would cause the body to acquire a terminal velocity, which might be observable. More likely to be important is relaxation to thermal equilibrium, which can still lead to a readily observable terminal velocity. A general treatment of such forces on a moving body, expressed in momentum space, is provided, which incorporates both propulsive and frictional forces. The source of the propulsive force is the nonsymmetric pattern of radiation from different parts of the body, the higher reflectivity of the metal portion playing a crucial role.

I. INTRODUCTION

The subject of quantum vacuum forces on neutral particles or bodies has a long history. The classic analysis of Einstein and Hopf [1] shows that a body moving nonrelativistically through vacuum experiences a frictional force opposing its motion that depends on the temperature of the environment. Dissipation is required, which may arise either from intrinsic processes within the body, producing an imaginary part of the electric susceptibility of the constituent material, or from the radiation field itself. For a short representative list of papers on quantum vacuum friction, see Refs. [2–7].

Much more work has been done on quantum electrodynamic friction near dissipative surfaces; for example, see Refs. [8–26]. In particular, attention has been directed to the force on a body or particle moving parallel to a dielectric or conducting surface. This configuration will typically give rise to a much larger frictional force, although even such friction has yet to be observed in the laboratory. These are nonequilibrium processes, but usually a non-equilibrium steady state (NESS) configuration has been considered, where the moving object neither gains nor loses energy, but absorbs momentum from the radiation field. This automatically happens if the body is nondissipative, with the radiation field being the only source of dissipation. If the body is dissipative, satisfaction of the NESS condition means that the temperature of the body bears a definite ratio to that of the environment, that ratio depending of the velocity of the body. For low velocities, where NESS reduces to thermal equilibrium, the ratio of temperatures tends to unity.

We recently revisited the subject of quantum vacuum friction, considering the relativistic regime and nonequilibrium phenomena [27, 28]. We proposed that the NESS temperature ratio might be an accessible signature for experimentally observing such effects. We considered both dipole fluctuations and field fluctuations as sources for the dissipative effects.

But, even more remarkably, fluctuation phenomena may lead to spontaneous torques and forces on stationary bodies out of equilibrium with their environment [29–40]. These effects, breaking time-reversal symmetry, typically require that the bodies be constituted of nonreciprocal material, that is, that the electric susceptibility be non-Hermitian.¹

* kmilton@ou.edu

† nima.pourtolami@gmail.com

‡ g.kennedy@soton.ac.uk

¹ For much more on nonreciprocal materials, see Ref. [41].

This may be achieved through the application of an external magnetic field; see, for example, Ref. [36]. We explored such anomalous torques and forces in a recent paper [42]; see also Ref. [43]. The effects considered there were first-order in the susceptibility or the polarizability. Although vacuum torques were found, no self-propulsive forces could appear in first order, unless the body were adjacent to another body, a dielectric or metal slab, for example.

To obtain a vacuum force for a body at rest requires not only nonequilibrium, but also nonuniformity of the electric susceptibility, although not necessarily nonreciprocity [44, 45]. This requires going to second order in the susceptibility. Even if the body is spatially nonsymmetric but possesses uniform susceptibility, no spontaneous force can arise, although it is claimed that a torque for such a body can appear if axial symmetry is broken, as for a pinwheel [44]. (We will explore the quantum vacuum torque in a subsequent paper.) In this paper, we demonstrate that a net force emerges if the susceptibility is nonuniform across the object. We analyze the general situation for an arbitrary susceptibility (Sec. II), and apply the analysis to four particular configurations: an inhomogeneous needle (Sec. III); an inhomogeneous spherical shell (Sec. IV); a ball with two halves made of different materials (a “Janus ball”) [44] (Sec. V); and a thin plate consisting of metal on one side and blackbody material² on the other (Sec. VI). Of course, once a body is set in motion, a frictional force will arise, resulting, eventually, in the body reaching a terminal velocity if the friction is large enough; this is explored in Sec. VII. However, it is likely that thermal relaxation effects will be much more important, and we show in Sec. VIII that these might still result in an readily observable terminal velocity. An outlook is provided in the Conclusions. Appendix A provides a momentum-space treatment of the spontaneous force, and shows how second-order friction emerges naturally. The thermal radiation from the body is analyzed more fully in Appendix B; the nonsymmetric thermal radiation pattern is responsible for the propulsive force. An explicit example of a dilute dielectric body attached to a perfectly reflective mirror is given in Appendix C.

II. SELF-PROPELLING FORCE

We follow the procedure detailed in Ref. [42, 43], where we studied only nonreciprocal bodies and worked only to first order in susceptibility, and found spontaneous torques, but no vacuum self-propulsive force.

We started with the formula for the Lorentz force on a dielectric body [Eq. (7.1) of Ref. [42]]:³

$$\mathbf{F} = \int(d\mathbf{r}) \int \frac{d\omega}{2\pi} \frac{d\nu}{2\pi} e^{-i(\omega+\nu)t} \left\{ -\left(1 + \frac{\omega}{\nu}\right) [\nabla \cdot \mathbf{P}(\mathbf{r}; \omega)] \mathbf{E}(\mathbf{r}; \nu) - \frac{\omega}{\nu} \mathbf{P}(\mathbf{r}; \omega) \cdot (\nabla) \cdot \mathbf{E}(\mathbf{r}; \nu) \right\}. \quad (2.1)$$

Here, the first term will not contribute to the corresponding quantum force, because the expectation value will make the sum of the frequencies vanish, $\omega + \nu = 0$. [See Eq. (2.4) below.] Then, as in the application of the principle of virtual work employed in Refs. [27, 28], we see that the force density may be thought of as the negative gradient of the interaction (free) energy density,

$$\mathfrak{f} = -\mathbf{P}(\mathbf{r}, t) \cdot \mathbf{E}(\mathbf{r}, t), \quad (2.2)$$

where the gradient acts only on the second, \mathbf{E} , factor. In Ref. [42] we expanded, to first order, the electric field in terms of the electric polarization,

$$\mathbf{E}^{(1)}(\mathbf{r}; \nu) = \int(d\mathbf{r}') \mathbf{\Gamma}(\mathbf{r}, \mathbf{r}'; \nu) \cdot \mathbf{P}(\mathbf{r}'; \nu), \quad (2.3a)$$

where $\mathbf{\Gamma}$ is the retarded electromagnetic Green’s dyadic, or we expanded the polarization in terms of the electric field,

$$\mathbf{P}^{(1)}(\mathbf{r}; \omega) = \boldsymbol{\chi}(\mathbf{r}; \omega) \cdot \mathbf{E}(\mathbf{r}; \omega), \quad (2.3b)$$

where $\boldsymbol{\chi} = \boldsymbol{\epsilon} - \mathbf{1}$ is the (local) electric susceptibility of the body.

In Ref. [42], we found a torque on a nonreciprocal body. We did so by applying the fluctuation-dissipation theorem (FDT) to evaluate field products:

$$\langle \mathcal{S}E_i(\mathbf{r}; \omega)E_j(\mathbf{r}'; \nu) \rangle = 2\pi\delta(\omega + \nu)(\Im\mathbf{\Gamma})_{ij}(\mathbf{r}, \mathbf{r}'; \omega) \coth \frac{\beta\omega}{2}, \quad \beta = \frac{1}{T}, \quad (2.4a)$$

$$\langle \mathcal{S}P_i(\mathbf{r}; \omega)P_j(\mathbf{r}'; \nu) \rangle = 2\pi\delta(\omega + \nu)\delta(\mathbf{r} - \mathbf{r}')(\Im\boldsymbol{\chi})_{ij}(\mathbf{r}; \omega) \coth \frac{\beta'\omega}{2}, \quad \beta' = \frac{1}{T'}, \quad (2.4b)$$

² By blackbody material we mean a substance whose mean electric polarizability per unit surface area is such as to yield the Planck spectrum and Stefan’s law. See Sec. VI.

³ The notation used in the second term here indicates, for its i th component, $P_j \nabla_i E_j$.

where \mathcal{S} denotes a symmetrized product, and \Im signifies the anti-Hermitian part, to obtain first-order effects. Here, T is the temperature of the blackbody background, while T' is that of the body. But there is, in vacuum, no first-order force, because the gradient of the Green's dyadic is then evaluated at coincident points.

In the current paper, we consider second-order effects. Iterating Eqs. (2.3a) and (2.3b) results in

$$\mathbf{E}^{(2)}(\mathbf{r}; \nu) = \int (d\mathbf{r}') \mathbf{\Gamma}(\mathbf{r}, \mathbf{r}'; \nu) \cdot \boldsymbol{\chi}(\mathbf{r}'; \nu) \cdot \mathbf{E}(\mathbf{r}'; \nu), \quad (2.5a)$$

$$\mathbf{E}^{(3)}(\mathbf{r}; \nu) = \int (d\mathbf{r}')(d\mathbf{r}'') \mathbf{\Gamma}(\mathbf{r}, \mathbf{r}'; \nu) \cdot \boldsymbol{\chi}(\mathbf{r}'; \nu) \cdot \mathbf{\Gamma}(\mathbf{r}', \mathbf{r}''; \nu) \cdot \mathbf{P}(\mathbf{r}''; \nu), \quad (2.5b)$$

$$\mathbf{P}^{(2)}(\mathbf{r}; \omega) = \int (d\mathbf{r}') \boldsymbol{\chi}(\mathbf{r}; \omega) \cdot \mathbf{\Gamma}(\mathbf{r}, \mathbf{r}'; \omega) \cdot \mathbf{P}(\mathbf{r}'; \omega), \quad (2.5c)$$

$$\mathbf{P}^{(3)}(\mathbf{r}; \omega) = \int (d\mathbf{r}') \boldsymbol{\chi}(\mathbf{r}; \omega) \cdot \mathbf{\Gamma}(\mathbf{r}, \mathbf{r}'; \omega) \cdot \boldsymbol{\chi}(\mathbf{r}'; \omega) \cdot \mathbf{E}(\mathbf{r}'; \omega), \quad (2.5d)$$

the order referring to the number of susceptibility factors, either $\boldsymbol{\chi}$ or $\mathbf{\Gamma}$. The second-order terms in the interaction energy (fourth order in susceptibilities) are obtained by using (1) $\mathbf{P}^{(0)}$ and $\mathbf{E}^{(3)}$, (2) $\mathbf{P}^{(2)}$ and $\mathbf{E}^{(1)}$, both of which give quadratic structures in \mathbf{P} , while quadratic structures in \mathbf{E} emerge by using (3) $\mathbf{P}^{(1)}$ and $\mathbf{E}^{(2)}$, and (4) $\mathbf{P}^{(3)}$ and $\mathbf{E}^{(0)}$. The FDT (2.4b) is applied for the former, while the FDT (2.4a) is applied for the latter. The resulting terms in the force will be denoted $\mathbf{F}^{(0,3)}$, $\mathbf{F}^{(2,1)}$, $\mathbf{F}^{(1,2)}$, and $\mathbf{F}^{(3,0)}$, respectively, in an obvious notation.

The EE fluctuations give rise to a force contribution in the z direction of

$$F_z^{\text{EE}} = \int (d\mathbf{r})(d\mathbf{r}') \frac{d\omega}{2\pi} \chi_{ij}(\mathbf{r}; \omega) \left[\nabla_z \Gamma_{ik}(\mathbf{r}, \mathbf{r}'; -\omega) \chi_{kl}(\mathbf{r}'; -\omega) (\Im \Gamma)_{jl}(\mathbf{r}, \mathbf{r}'; \omega) \right. \\ \left. + \Gamma_{jk}(\mathbf{r}, \mathbf{r}'; \omega) \chi_{kl}(\mathbf{r}'; \omega) \nabla_z (\Im \Gamma)_{li}(\mathbf{r}', \mathbf{r}; \omega) \right] \coth \frac{\beta\omega}{2}, \quad (2.6a)$$

while the PP fluctuations give

$$F_z^{\text{PP}} = \int (d\mathbf{r})(d\mathbf{r}') \frac{d\omega}{2\pi} \nabla_z \Gamma_{jk}(\mathbf{r}, \mathbf{r}'; -\omega) \left[\chi_{kl}(\mathbf{r}'; -\omega) \Gamma_{lm}(\mathbf{r}', \mathbf{r}; -\omega) (\Im \chi)_{jm}(\mathbf{r}; \omega) \right. \\ \left. + (\Im \chi)_{mk}(\mathbf{r}'; \omega) \Gamma_{lm}(\mathbf{r}, \mathbf{r}'; \omega) \chi_{jl}(\mathbf{r}; \omega) \right] \coth \frac{\beta'\omega}{2}. \quad (2.6b)$$

Equation (2.6a) displays the (1,2) and (3,0) contributions, respectively, while Eq. (2.6b) displays the (0,3) and (2,1) contributions, respectively.

Henceforth, we restrict attention to reciprocal bodies. The general result is particularly simple if the susceptibility is isotropic,

$$\chi_{ij}(\mathbf{r}; \omega) = \delta_{ij} \chi(\mathbf{r}; \omega), \quad (2.7)$$

and the background is not only reciprocal,

$$\Gamma_{ij}(\mathbf{r}, \mathbf{r}'; \omega) = \Gamma_{ji}(\mathbf{r}', \mathbf{r}; \omega), \quad (2.8)$$

but also homogeneous, in which case the Green's dyadic is a function only of $\mathbf{R} = \mathbf{r} - \mathbf{r}'$. We then use symmetry under $\mathbf{r} \leftrightarrow \mathbf{r}'$ and also $\omega \rightarrow -\omega$, noting that the imaginary part of the susceptibility is odd in ω , to derive the quantum vacuum force in the z -direction, which is, including the contributions from EE and PP fluctuations,

$$F_z = \int (d\mathbf{r})(d\mathbf{r}') \int_{-\infty}^{\infty} \frac{d\omega}{2\pi} X(\mathbf{r}, \mathbf{r}'; \omega) \text{Im} \Gamma_{ji}(\mathbf{r}' - \mathbf{r}; \omega) \nabla_z \text{Im} \Gamma_{ij}(\mathbf{r} - \mathbf{r}'; \omega) \left[\coth \frac{\beta\omega}{2} - \coth \frac{\beta'\omega}{2} \right], \quad (2.9)$$

where the second-order susceptibility product is

$$X(\mathbf{r}, \mathbf{r}'; \omega) = \text{Im} [\chi(\mathbf{r}; \omega) \chi(\mathbf{r}'; \omega)^*] = \text{Im} \chi(\mathbf{r}; \omega) \text{Re} \chi(\mathbf{r}'; \omega) - \text{Re} \chi(\mathbf{r}; \omega) \text{Im} \chi(\mathbf{r}'; \omega). \quad (2.10)$$

(Note that only the first term of Eq (2.6a), $F^{(1,2)}$, contributes in the isotropic case, because the integrand of the second term is antisymmetric under $\mathbf{r} \leftrightarrow \mathbf{r}'$.) It is clear that if the susceptibility of the body is homogeneous, so χ is independent of \mathbf{r} within the body, the force is zero, since $X = 0$ then. So, we need an inhomogeneous body in order to generate a spontaneous quantum vacuum force.

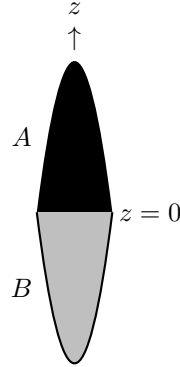


FIG. 1. Cartoon of the inhomogeneous bodies considered in this paper. The upper part, A , will typically be a (nondispersive) insulator, while the lower part, B , will be a Drude-type metal. The figure is intended to illustrate a solid body, rotationally invariant about the z -axis. Because of this symmetry, the force must be either parallel or antiparallel to the z -axis.

The next simplest possibility is to imagine the object as consisting of two separate parts, labeled A and B , in each of which χ is spatially constant, as illustrated in Fig. 1. Then the formula for the force reduces to

$$F_z = 8 \int_0^\infty \frac{d\omega}{2\pi} X_{AB}(\omega) \left[\frac{1}{e^{\beta\omega} - 1} - \frac{1}{e^{\beta'\omega} - 1} \right] I_{AB}(\omega), \quad (2.11a)$$

where

$$I_{AB}(\omega) = \int_A (d\mathbf{r}) \int_B (d\mathbf{r}') \frac{1}{2} \nabla_z [\text{Im} \Gamma_{ji}(\mathbf{r}', \mathbf{r}; \omega) \text{Im} \Gamma_{ij}(\mathbf{r}, \mathbf{r}'; \omega)], \quad (2.11b)$$

and

$$X_{AB}(\omega) = \text{Im} \chi_A(\omega) \text{Re} \chi_B(\omega) - \text{Re} \chi_A(\omega) \text{Im} \chi_B(\omega). \quad (2.11c)$$

Since the divergenceless part⁴ of the vacuum Green's dyadic is

$$\mathbf{\Gamma}^{(0)\prime}(\mathbf{r} - \mathbf{r}'; \omega) = (\nabla \nabla - \mathbf{1} \nabla^2) \frac{e^{i\omega R}}{4\pi R} = [\hat{\mathbf{R}} \hat{\mathbf{R}} (3 - 3i\omega R - \omega^2 R^2) - \mathbf{1} (1 - i\omega R - \omega^2 R^2)] \frac{e^{i\omega R}}{4\pi R^3}, \quad (2.12)$$

where $R = |\mathbf{R}|$ and $\hat{\mathbf{R}} = \mathbf{R}/R$, and the matrix trace appearing in Eq. (2.11b) is

$$\text{Im} \Gamma_{ji}(-\mathbf{R}; \omega) \text{Im} \Gamma_{ij}(\mathbf{R}; \omega) = \frac{2\Delta(\omega R)}{(4\pi R^3)^2}, \quad (2.13a)$$

with

$$\Delta(\omega R) = (3 - 2\omega^2 R^2 + \omega^4 R^4) \sin^2 \omega R - \omega R (3 - \omega^2 R^2) \sin 2\omega R + 3\omega^2 R^2 \cos^2 \omega R. \quad (2.13b)$$

Note that this trace is finite as $R \rightarrow 0$ since

$$\Delta(u) \sim \frac{2}{3}u^6 - \frac{2}{9}u^8 + \dots, \quad u \ll 1. \quad (2.14a)$$

Although it therefore appears that the leading term, proportional to u^6 , never contributes to the geometrical integral (2.11b), this depends on the convergence of the integrals—see Sec. VI B. And, apart from subdominant oscillating terms, the large-argument behavior is

$$\Delta(u) \sim \frac{1}{2}u^4 + \dots, \quad u \gg 1. \quad (2.14b)$$

An alternative, momentum-space formulation, of the force appears in Appendix A.

⁴ The divergenceless part of the Green's dyadic is defined by $\mathbf{\Gamma}' = \mathbf{\Gamma} + \mathbf{1}$, where $\mathbf{1}$ includes a spatial delta function.

III. INHOMOGENEOUS NEEDLE

This simplest example is a one-dimensional needle, lying along the z -axis, with one side being made of uniform material A , and of length a ; and the other side of uniform material B , and of length b :

$$\chi(\mathbf{r}; \omega) = C [\delta(x)\delta(y)\theta(z)\theta(a-z)\chi_A(\omega) + \delta(x)\delta(y)\theta(-z)\theta(b+z)\chi_B(\omega)], \quad (3.1)$$

for the needle having constant (small) cross-sectional area C . Then, the double volume integral I_{AB} just involves $R = z' - z$ ($z' > 0 > z$), and can be explicitly evaluated:

$$I_{AB} = \frac{C^2 \omega^5}{(4\pi)^2} [f(\omega(a+b)) - f(\omega a) - f(\omega b)], \quad (3.2)$$

where

$$f(x) = \frac{1}{30x^5} g(x), \quad (3.3a)$$

with

$$g(x) = -9 - 5x^2(1 + 3x^2) + (9 - 13x^2 + 11x^4) \cos 2x + 2x(9 - x^2) \sin 2x + 22x^5 \text{Si}(2x). \quad (3.3b)$$

Here, the sine integral function is defined by

$$\text{Si}(x) = \int_0^x \frac{dt}{t} \sin t. \quad (3.4)$$

The behavior of the function g for small and large arguments is

$$g(x) \sim 20x^6 - \frac{20}{9}x^8 \quad \text{as } x \rightarrow 0, \quad (3.5a)$$

and

$$g(x) \sim 11\pi x^5 \quad \text{as } x \rightarrow \infty. \quad (3.5b)$$

Thus, the self-propulsive force (2.11a) on the needle can be written as

$$F_z = \frac{C^2}{2\pi^3} \int_0^\infty d\omega \omega^5 X_{AB}(\omega) \left[\frac{1}{e^{\beta\omega} - 1} - \frac{1}{e^{\beta'\omega} - 1} \right] [f(\omega(a+b)) - f(\omega a) - f(\omega b)]. \quad (3.6)$$

One curious feature is immediately apparent: For high temperatures, or $\beta, \beta' \ll 1$, the frequency integral should be dominated by large values of ω , where $f(x) \sim 11/30$ is independent of x . Thus, in this limit, the force is independent of the dimensions of the needle; that is, only a relatively small region of the needle near the intersection of the two halves contributes to the force. At room temperature, this independence of the size of the needle should hold if $a, b \gg 10 \mu\text{m}$. For low temperatures, or $\beta, \beta' \gg 1$, low values of ω should dominate, and in view of the behavior in Eq. (3.5a), the leading term in g will give no contribution to the force, as already recognized above, and the second term will yield bilinear behavior, that is $F_z \propto ab$.

Now let us compute the force for a situation with χ_A being a real constant (because the frequencies involved should be small compared to the atomic binding energies—but see the discussion at the end of Sec. V), while χ_B is given by the Drude model, which is a good approximation for a metal:

$$\chi_B(\omega) = -\frac{\omega_p^2}{\omega^2 + i\omega\nu}, \quad (3.7)$$

where ω_p is the plasma frequency and ν is the damping parameter, about 9 eV and 0.035 eV, respectively, for gold. Let us express the dimensional quantities in terms of reference scales, β_0 and a_0 . For numerical work we will take $\beta_0 = 40 \text{ (eV)}^{-1}$, corresponding to room temperature, and a macroscopic size $a_0 = 1 \text{ cm}$. For these values, the dimensionless ratio is $a_0/\beta_0 = 1250$. Then, with

$$\beta = \hat{\beta}\beta_0, \quad \beta' = \hat{\beta}'\beta_0, \quad \beta_0\omega = y, \quad \beta_0\nu = \lambda, \quad (3.8)$$

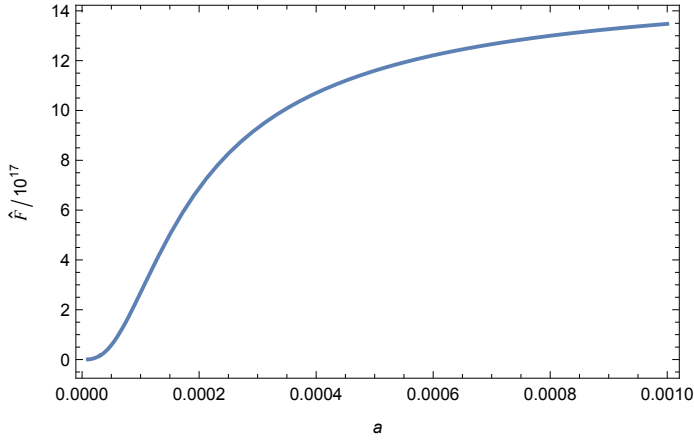


FIG. 2. Dimensionless force \hat{F} on an inhomogeneous needle with $a = b$ as a function of a for $T = 300$ K and $T' = 600$ K. The half-length of the needle is given in cm.

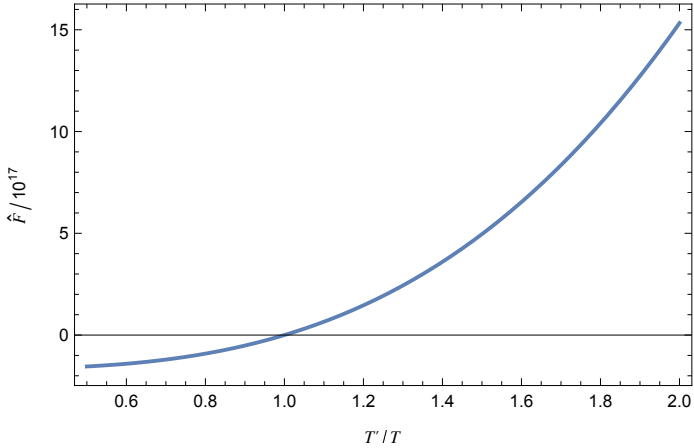


FIG. 3. Dimensionless force \hat{F} on an inhomogeneous needle with $a = b$ as a function of T' for $T = 300$ K. The half-length of the needle is taken to be 1 cm.

we define

$$h(u, \hat{\beta}) = \frac{1}{u^5} \int_0^\infty \frac{dy}{y} \frac{1}{y^2 + \lambda^2} g\left(\frac{a_0}{\beta_0} y u\right) \frac{1}{e^{\hat{\beta} y} - 1}, \quad (3.9)$$

in terms of which the force is

$$F = -\frac{C^2 \omega_p^2 \nu \chi_A}{60\pi^3} \frac{\beta_0^2}{a_0^5} \hat{F}, \quad (3.10a)$$

where

$$\hat{F} = h\left(\frac{a+b}{a_0}, \hat{\beta}\right) - h\left(\frac{a}{a_0}, \hat{\beta}\right) - h\left(\frac{b}{a_0}, \hat{\beta}\right) - h\left(\frac{a+b}{a_0}, \hat{\beta}'\right) + h\left(\frac{a}{a_0}, \hat{\beta}'\right) + h\left(\frac{b}{a_0}, \hat{\beta}'\right). \quad (3.10b)$$

We now show numerical results. We take the above stated parameters so, for gold, $\lambda = 1.4$, and the magnitude of the prefactor in the force (3.10b) is $3.85\chi_A \times 10^{-20}$ N if the cross-sectional radius of the needle is 1 mm. Figure 2 shows the saturation of the force at a value of about 0.06 N for large a . The figure also shows how the force vanishes for small a . Finally, the temperature dependence is sketched in Fig. 3.

However, this is likely to be a gross overestimate. Because the metal has a small skin depth, which we estimate in terms of the conductivity σ as follows,

$$\delta = (\omega\sigma/2)^{-1/2} = (\omega^2 \text{Im } \chi/2)^{-1/2} = \sqrt{\frac{2(\omega^2 + \nu^2)}{\omega\omega_p^2\nu}}, \quad (3.11)$$

which, for our nominal values and for $\omega \sim \beta_0^{-1}$, turns out to be of order 50 nm. So, the force on a needle with this tiny cross section, rather than one of 1 mm radius, would be reduced by a factor of $\sim 10^{-18}$. Interestingly, since $1/\beta_0$ and ν are comparable, the skin depth is near its minimal value, achieved when $\omega = \nu$, $\delta_{\min} = 2/\omega_p$.

The reason the force is toward the metal end of the needle (negative in our convention) might seem to be that emissivity of a metal is far lower than that of an insulator, so there is more radiant energy emitted from the insulator end of the needle. The corresponding momentum imbalance drives the object in the $-z$ direction. However, this is not quite borne out by our perturbative calculations, which show, for modest temperatures, more thermal radiation is emitted by the metal than by the dielectric. However, the emission from the dielectric is nearly entirely reflected by the metal, so the momentum imbalance remains the same. An explicit example of this is detailed in Appendix C.

IV. THIN SPHERICAL SHELL

In view of the preceding remarks concerning skin depth, we next consider a spherical shell, with thickness t , smaller than the skin depth, and much smaller than the radius a of the sphere. We imagine that the sphere is inhomogeneous: in terms of the polar angle θ ,

$$\chi(\mathbf{r}; \omega) = \begin{cases} 0 < \theta < \frac{\pi}{2} : \chi_A(\omega), \\ \frac{\pi}{2} < \theta < \pi : \chi_B(\omega). \end{cases} \quad (4.1)$$

The square of the distance between two points on the two hemispheres is given by

$$R^2 = 2a^2(1 - \cos \gamma) = 2a^2[1 - \cos \theta \cos \theta' - \sin \theta \sin \theta' \cos(\phi - \phi')], \quad (4.2)$$

where γ is the angle between two points, one on the upper hemisphere and one on the lower. Then, the geometrical integral is

$$I_{AB} = \int_A (d\mathbf{r}) \int_B (d\mathbf{r}') \partial_z \left[\frac{\Delta(\omega R)}{(4\pi R^3)^2} \right] = \frac{\omega^8 a}{(4\pi)^2} \int_A (d\mathbf{r}) \int_B (d\mathbf{r}') \frac{\cos \theta - \cos \theta'}{u} D(u), \quad (4.3)$$

where $u = \omega R$. The u derivative occurring here is explicitly

$$D(u) = \frac{\partial}{\partial u} \left[\frac{\Delta(u)}{u^6} \right] = \frac{1}{u^7} [-9 - u^2(2 + u^2) + (9 - 16u^2 + 3u^4) \cos 2u + u(18 - 8u^2 + u^4) \sin 2u], \quad (4.4)$$

which behaves as

$$D(u) \sim -\frac{4}{9}u, \quad u \rightarrow 0, \quad (4.5a)$$

$$D(u) \sim -\frac{1}{u^3} + \frac{\sin(2u)}{u^2}, \quad u \rightarrow \infty. \quad (4.5b)$$

The low- u behavior follows from Eq. (2.14a), where again we note that the u^6 term does not contribute. The last term for large u rapidly oscillates, and on the average gives a term of $O(u^{-4})$, so is subdominant.

For our inhomogeneous sphere, with vanishing thickness t , the geometrical integral is a threefold one:

$$I_{AB} = \frac{\omega^8 a^5 t^2}{8\pi} \mathcal{I}_{AB}(\omega a), \quad (4.6a)$$

with

$$\mathcal{I}_{AB}(\omega a) = \int_0^{\pi/2} d\theta \sin \theta \int_0^{2\pi} d\phi \int_{\pi/2}^{\pi} d\theta' \sin \theta' (\cos \theta - \cos \theta') \frac{D(u)}{u}. \quad (4.6b)$$

For a macroscopic object, one would think that the large u behavior of D is dominant, because for a 1 cm sphere at room temperature the characteristic value of $\omega a \sim 1250$. But this might be misleading, since polar angles close to the equator of the sphere correspond to $\gamma \rightarrow 0$. In Fig. 4 we show the result of numerical integration, and compare with that arising from the leading large- u behavior.

Using the result of the approximate fit for \mathcal{I}_{AB} , and the model we used for the needle, that $\chi_A(\omega)$ is constant and χ_B is given by the Drude model (3.7), we find for the self-propulsive force (2.11a)

$$F = -\frac{\omega_p^2 t^2 a}{16\pi^2} \chi_A \nu^3 \mathcal{N} \hat{F}, \quad (4.7a)$$

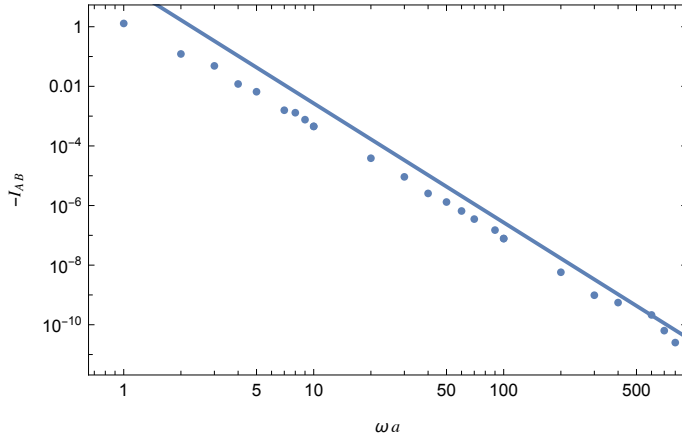


FIG. 4. The integral $-\mathcal{I}_{AB}$ in Eq. (4.6b), evaluated numerically (blue dots), The line shows the result of replacing $D(u)$ by its asymptotic value $-\frac{1}{u^3}$, which is exactly described by a power law $(\omega a)^{-4}$. The coefficient of the fit to \mathcal{I}_{AB} is $\mathcal{N} = -26.88$. The “exact” results exhibit considerable scatter, only part of which reflects the serious oscillations of the integrand; the numerical integration becomes unstable for large values of ωa . Although those points lie below the asymptotic line, they seem to be approaching it.

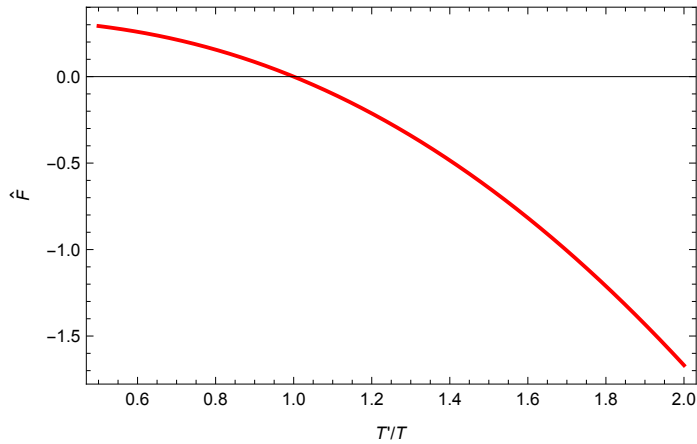


FIG. 5. Dimensionless force on an inhomogeneous sphere with the northern hemisphere having a constant susceptibility, and the southern hemisphere being a Drude metal, with the environment being at room temperature, for various values of the temperature of the sphere, T' . The prefactor in the force (4.7a), for our nominal values for gold, and the minimum value of the skin depth, $t = 2/\omega_p$, is $1.2 \times 10^{-12} \chi_A$ N, for a sphere of 1 cm radius. The force is computed in the approximation that the geometric integral I_{AB} is described by the fit to the large- u asymptotics in Fig. 4.

where

$$\hat{F} = \int_0^\infty dx \frac{x^3}{x^2 + 1} \left(\frac{1}{e^{\beta \nu x} - 1} - \frac{1}{e^{\beta' x \nu} - 1} \right), \quad (4.7b)$$

the integrals being explicitly

$$\int_0^\infty dx \frac{x^3}{x^2 + 1} \frac{1}{e^{xy} - 1} = \frac{\pi^2}{6y^2} - \frac{1}{2} \left[\ln \left(\frac{y}{2\pi} \right) - \frac{\pi}{y} - \psi \left(\frac{y}{2\pi} \right) \right]. \quad (4.8)$$

The dimensionless force \hat{F} is plotted in Fig. 5.

V. JANUS BALL

We now turn to what has been called a Janus ball, a spherical volume with the forward and rear halves composed of different homogeneous materials. In view of our previous remarks about skin depth, we should restrict attention

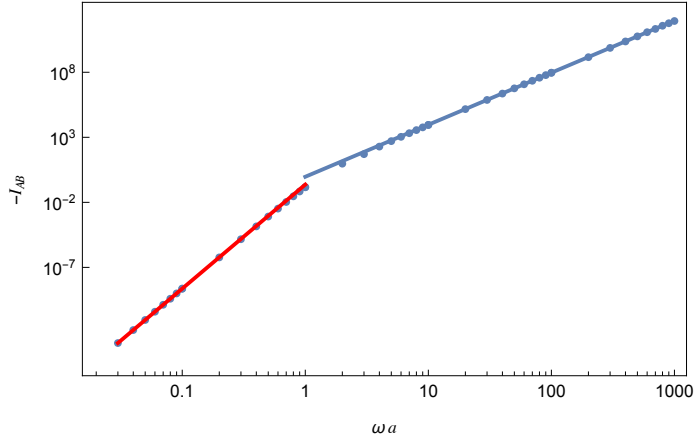


FIG. 6. The dots show the results of numerical integration of the two four-fold integrals in (5.2b). Shown is the magnitude of the difference of the two integrals. The upper line (blue) is the large- u asymptotic behavior resulting from (2.14b), that is, $\mathcal{I}_{AB} \sim -0.927(\omega a)^4$. The fit is very good for values of $\omega a > 10$. Values of ωa smaller than 1 are well described by $\mathcal{I}_{AB} \sim -\frac{2\pi}{27}(\omega a)^8$, which results from the u^8 term in Eq. (2.14a), the u^6 term never contributing.

to a nanometer-sized object. Because I_{AB} is the integral of a gradient, the double radial integral becomes a surface integral,

$$I_{AB} = \int_{S_A} d\mathbf{S} \cdot \hat{\mathbf{z}} \int_B (dr') \frac{\Delta(\omega R)}{(4\pi R^3)^2}, \quad (5.1)$$

where S_A is the surface of the A half-ball, that is, a hemisphere of radius a , $0 < \theta < \frac{\pi}{2}$ and a disk $\theta = \pi/2$, $0 \leq r \leq a$, while the second integral is over the volume of the lower B half-ball, for polar angle $\frac{\pi}{2} > \theta > \pi$. Explicitly, the integral can be written in two parts:

$$I_{AB} = \frac{1}{8\pi a} \mathcal{I}_{AB}, \quad (5.2a)$$

with

$$\begin{aligned} \mathcal{I}_{AB} = & \int_0^{\pi/2} d\theta \sin \theta \cos \theta \int_0^1 d\rho' \rho'^2 \int_{\pi/2}^{\pi} d\theta' \sin \theta' \int_0^{2\pi} d\phi' \frac{\Delta(\omega a P_1)}{P_1^6} \\ & - \int_0^1 d\rho \rho \int_0^1 d\rho' \rho'^2 \int_{\pi/2}^{\pi} d\theta' \sin \theta' \int_0^{2\pi} d\phi' \frac{\Delta(\omega a P_2)}{P_2^6}, \end{aligned} \quad (5.2b)$$

where $\rho = r/a$, $\rho' = r'/a$, and

$$P_1^2 = 1 + \rho'^2 - 2\rho'(\cos \theta \cos \theta' + \sin \theta \sin \theta' \cos \phi'), \quad (5.3a)$$

$$P_2^2 = \rho^2 + \rho'^2 - 2\rho\rho' \sin \theta' \cos \phi', \quad (5.3b)$$

because on the bisecting disk, $\theta = \pi/2$. Once these four-fold integrals are done, the force, for the same model considered above, is obtained from

$$F = -\frac{\omega_p^2 \epsilon}{2\pi^2} \chi_A \int_0^\infty du \frac{1}{u(u^2 + \epsilon^2)} \mathcal{I}_{AB}(u) \left[\frac{1}{e^{\beta u/a} - 1} - \frac{1}{e^{\beta' u/a} - 1} \right], \quad (5.4)$$

in terms of the abbreviations $\epsilon = \nu a$, $u = \omega a$.

Numerical integration of the two integrals in Eq. (5.2b) is shown in Fig. 6. The figure shows that for large values of ωa , appropriate to a macroscopic ball near room temperature, the linear fit from the large u behavior of $\Delta(u)$ in Eq. (2.14b) is quite good, and results in the following behavior of I_{AB} :

$$I_{AB}^{\text{JB}} \sim -\frac{1}{8\pi a} (0.927)(\omega a)^4. \quad (5.5)$$

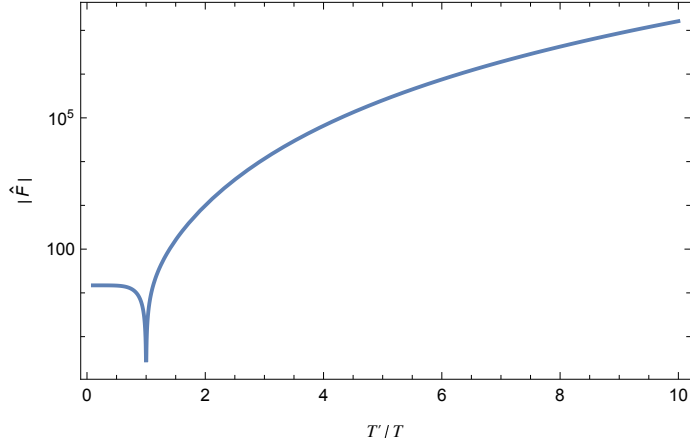


FIG. 7. Dimensionless force \hat{F} on a Janus ball composed of a northern hemisphere made of a dispersionless dielectric, and the southern hemisphere composed of a Drude metal. Parameters are as given in the text. The force, given by Eq. (5.7b), is plotted as a function of the temperature of the sphere, T' , for the temperature of the environment fixed at room temperature. The magnitude is shown in this log plot; the force is negative for $T' > T$.

This has the same ω dependence as that for a thin spherical shell in this limit, which, from Eq. (4.6a), is

$$I_{AB}^{\text{HS}} \sim -\frac{26.9}{8\pi} \omega^4 a t^2. \quad (5.6)$$

This will be the same as I_{AB}^{JB} if $a = 5.39t$. So apart from a factor of $0.035(a/t)^2$, the forces will be the same in the large a limit.

But as noted above, only the small sphere situation is likely to be physically relevant. For small a , the forces will have a different behavior. The lower (red) line in Fig. 6 is $\mathcal{I}_{AB} = -\frac{2\pi}{27}(\omega a)^8$, which follows from performing the elementary integrations occurring when Eq. (2.14a) holds: the u^6 term cancels between the disk and the hemisphere surface integrals (as noted above, the u^6 term never contributes), and the u^8 term gives the value stated. So for a small Janus ball the force is given by

$$F^{\text{JB}} = \frac{1}{27\pi} \chi_A \omega_p^2 (\nu a)^7 \hat{F}, \quad (5.7a)$$

where the dimensionless force is

$$\begin{aligned} \hat{F} &= \int_0^\infty dx \frac{x^7}{x^2 + 1} \left(\frac{1}{e^{\beta\nu x} - 1} - \frac{1}{e^{\beta'\nu x} - 1} \right) \\ &= -\frac{1}{2} \left[\ln \frac{T'}{T} + \frac{\pi}{\nu} (T' - T) + \psi \left(\frac{\nu}{2\pi T'} \right) - \psi \left(\frac{\nu}{2\pi T} \right) \right] \\ &\quad + \frac{\pi^2}{6} \frac{1}{\nu^2} (T^2 - T'^2) - \frac{\pi^4}{15} \frac{1}{\nu^4} (T^4 - T'^4) + \frac{8\pi^6}{63} \frac{1}{\nu^6} (T^6 - T'^6). \end{aligned} \quad (5.7b)$$

The absolute value of this function is plotted in Fig. 7, as a function of the body temperature T' , for the environment temperature $T = 300$ K, and $\nu = 0.035$ eV, appropriate for gold. If further the radius of the sphere is $1 \mu\text{m}$, the prefactor for a gold microsphere ($\omega_p = 9$ eV) is $3.84 \times 10^{-18} \chi_A$ N, so this might be observable. Note that the force is negative for $T' > T$, so it is in the direction of the metal end of the ball. These results are roughly consistent with those found in Ref. [44]. They consider a Janus ball with one half SiO_2 and the other half gold, and for $T = 0$ K and $T' = 300$ K find a force of about 4×10^{-18} N on a $1 \mu\text{m}$ ball. Here, for the same example, we find the prefactor in Eq. (5.7a) to be 3×10^{-18} N, while \hat{F} is about 15. A plot of \hat{F} for a vacuum environment at 0 K is shown in Fig. 8, again qualitatively similar to the results of Ref. [44]. However, the scaling with the radius of the ball is quite different: we find a a^7 behavior, whereas they report scaling roughly with the volume.

For sufficiently high temperatures, the dispersion of the dielectric cannot be ignored. Therefore, let use a more realistic Lorentzian model,

$$\chi_A(\omega) = \frac{\tilde{\omega}_p^2}{\omega_0^2 - \omega^2 - i\omega\gamma}. \quad (5.8)$$

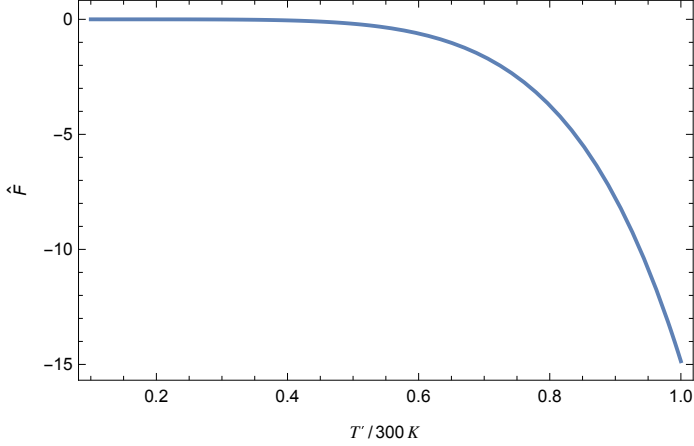


FIG. 8. Dimensionless force \hat{F} for a Janus ball composed of gold and SiO_2 , for the vacuum at zero temperature, as a function of the temperature of the ball.

Then, the second-order susceptibility factor that appears in the force is

$$X(\omega) = -\frac{\omega_p^2 \tilde{\omega}_p^2 [\omega_0^2 \nu + \omega^2 (\gamma - \nu)]}{[(\omega_0^2 - \omega)^2 + \omega^2 \gamma^2] [\omega(\omega^2 + \nu^2)]}. \quad (5.9)$$

Of course, this agrees with what we had previously if $\omega \ll \omega_0$, provided $\chi_A = \tilde{\omega}_p^2 / \omega_0^2$. The propulsive force is now

$$F = \frac{1}{27\pi} \omega_p^2 \tilde{\omega}_p^2 a^7 T^5 \hat{F}, \quad (5.10a)$$

the dimensionless force being

$$\hat{F} = \int_0^\infty dy y^7 \frac{y_0^2 \mu + y^2 (\mu - \lambda)}{[(y_0^2 - y^2)^2 + y^2 \mu^2] [y^2 + \lambda^2]} \left[\frac{1}{e^{y/t} - 1} - \frac{1}{e^{y/t'} - 1} \right], \quad (5.10b)$$

where in terms of the inverse of room temperature, β_0 , the dimensionless variables are

$$\lambda = \beta_0 \nu, \quad \mu = \beta_0 \gamma, \quad y_0 = \beta_0 \omega_0, \quad y = \beta_0 \omega, \quad t = \beta_0 T, \quad t' = \beta_0 T'. \quad (5.10c)$$

We illustrate the effect of this change on the force on a small Janus ball where $I_{AB} = -\frac{(\omega a)^8}{108a}$ in Fig. 9.

VI. BLACKBODY/METAL PLANAR SURFACE

A. Blackbody surface

We preface this section by considering the power absorbed by an object out of thermal equilibrium. In first order, the power is classically

$$P = \frac{\partial \mathcal{F}}{\partial t} = - \int (d\mathbf{r}) \mathbf{P}(\mathbf{r}, t) \cdot \frac{\partial}{\partial t} \mathbf{E}(\mathbf{r}, t). \quad (6.1)$$

We see here the reappearance of the (free) energy density (2.2). For an object at temperature T' in vacuum at temperature T , the FDT implies

$$P = \int (d\mathbf{r}) \frac{d\omega}{2\pi} \omega \text{Im} \chi_{ij}(\mathbf{r}; \omega) \text{Im} \Gamma_{ji}(\mathbf{r}, \mathbf{r}'; \omega) \bigg|_{\mathbf{r}' \rightarrow \mathbf{r}} \left[\coth \frac{\beta \omega}{2} - \coth \frac{\beta' \omega}{2} \right]. \quad (6.2)$$

For an isotropic body, $\chi_{ij}(\mathbf{r}; \omega) = \chi(\mathbf{r}; \omega) \delta_{ij}$, and a vacuum environment, where $\text{tr} \text{Im} \Gamma(\mathbf{r}, \mathbf{r}'; \omega) \big|_{\mathbf{r}=\mathbf{r}'} = \omega^3 / (2\pi)$, the power simplifies to

$$P = \frac{1}{\pi^2} \int (d\mathbf{r}) \int_0^\infty d\omega \omega^4 \text{Im} \chi(\mathbf{r}; \omega) \left[\frac{1}{e^{\beta \omega} - 1} - \frac{1}{e^{\beta' \omega} - 1} \right]. \quad (6.3)$$

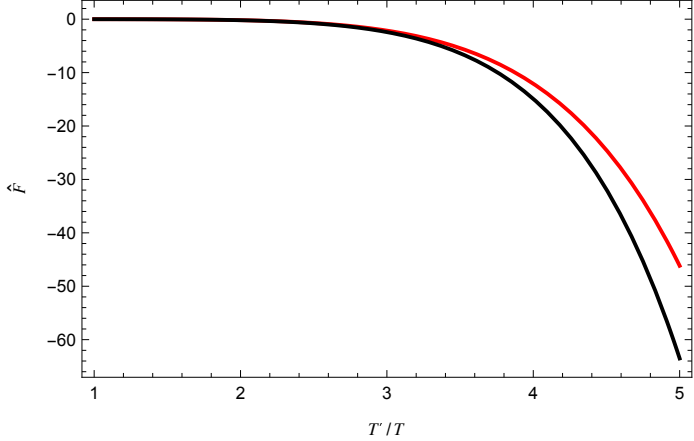


FIG. 9. Plot of the dimensionless force \hat{F} for a Janus ball with dielectric on the A side and metal on the B side, as a function of the temperature of the ball. The metal is chosen to be gold, for which $\mu = 1.4$, the dielectric is polystyrene, for which, roughly [47] (taking the first term in a four-term fit to the susceptibility) $y_0 = 240$ and $\lambda = 26$, and we consider a room-temperature background. The upper (red) curve assumes a dispersionless dielectric, while the lower (black) curve includes the single Lorentzian dispersion model. The effect of the latter is rather small, except at very high temperature.

Now the power absorbed by a blackbody is given by Stefan's law,

$$P = S \frac{\pi^2}{60} (T^4 - T'^4), \quad (6.4)$$

where S is the surface area of the blackbody. Since the radiation from a blackbody arises entirely from the surface, we can write

$$\int_V (d\mathbf{r}) \chi(\mathbf{r}; \omega) = \int_S dS \tilde{\chi}(\mathbf{r}; \omega), \quad (6.5)$$

so in order for Eq. (6.3) to describe a blackbody, the surface susceptibility must satisfy

$$\text{Im } \tilde{\chi}(\omega) = \frac{1}{4\omega} \Rightarrow \tilde{\chi}(\omega) = \frac{i}{4} \frac{1}{\omega + i\epsilon} = \frac{\pi}{4} \delta(\omega) + \mathcal{P} \frac{i}{4\omega}, \quad (6.6)$$

\mathcal{P} signifying the principal part, the latter following from the Kramers-Kronig relation.

B. Force on a blackbody/metal plate

Now we want to calculate the self-propulsive force on a composite plate consisting of a blackbody surface on one side and a Drude metal on the other. The force is given by Eq. (2.11a), in terms of the geometrical integral (2.11b),

$$I_{AB} = \int_A (d\mathbf{r}) \int_B (d\mathbf{r}') \nabla_z \frac{\Delta(\omega|\mathbf{r} - \mathbf{r}'|)}{(4\pi|\mathbf{r} - \mathbf{r}'|^3)^2}. \quad (6.7)$$

Using polar coordinates for the transverse spatial integrals, and integrating out the z derivative, we find for plates of (large) cross sectional area S and thicknesses of the two sides t_A and t_B , respectively,

$$\begin{aligned} I_{AB} &= \frac{S}{32\pi} \int_0^\infty \rho d\rho \int_{-t_B}^0 dz' \left[\frac{\Delta(\omega\sqrt{\rho^2 + (t_A - z')^2})}{(\rho^2 + (t_A - z')^2)^3} - \frac{\Delta(\omega\sqrt{\rho^2 + z'^2})}{(\rho^2 + z'^2)^3} \right] \\ &= \frac{S}{32\pi} \int_{-t_B}^0 dz' \int_{t_A - z'}^{-z'} du \frac{\Delta(\omega u)}{u^5}. \end{aligned} \quad (6.8)$$

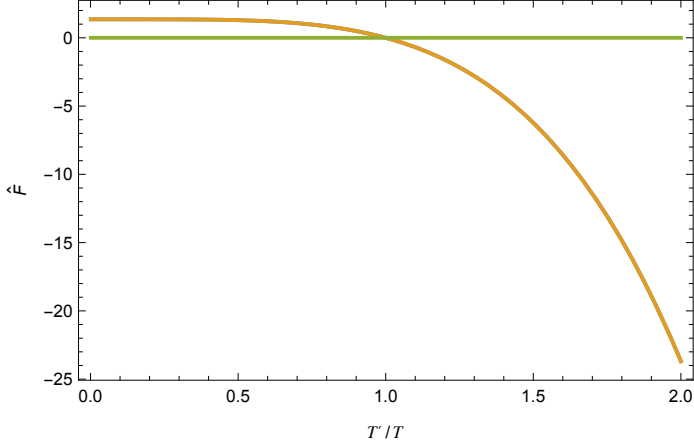


FIG. 10. Dimensionless force (6.14b) on a thin plate consisting of a blackbody on the positive- z side and a Drude metal on the negative- z side.

Because $\omega \sim T$, T' corresponds to a length scale $\sim 10 \mu\text{m}$ for temperatures around room temperature, for thicknesses much smaller than that, we can expand $\Delta(\omega u)$ using only the first term in Eq. (2.14a), and then we obtain immediately⁵

$$I_{AB} = -\frac{S}{96\pi} t_A t_B (t_A + t_B) \omega^6. \quad (6.11)$$

Then the force is given by

$$F_z = -\frac{S}{24\pi^2} t_A t_B (t_A + t_B) \int_0^\infty d\omega \hat{\chi}_{AB}(\omega) \omega^6 \left[\frac{1}{e^{\beta\omega} - 1} - \frac{1}{e^{\beta'\omega} - 1} \right]. \quad (6.12)$$

When A is the blackbody, $t_A \text{Im} \chi_A = \frac{1}{4\omega}$, while B is the Drude metal, described by Eq. (3.7), the force is

$$F_z = \frac{St_B(t_A + t_B)}{96\pi^2} \omega_p^2 \int_0^\infty d\omega \frac{\omega^5}{\omega^2 + \nu^2} \left[\frac{1}{e^{\beta\omega} - 1} - \frac{1}{e^{\beta'\omega} - 1} \right]. \quad (6.13)$$

Again, this is of the same class of functions explored in Appendix A of Ref. [42],

$$F_z = \frac{St_B(t_A + t_B) \omega_p^2 \nu^4}{96\pi^2} \hat{F}, \quad (6.14a)$$

where

$$\begin{aligned} \hat{F} &= \int_0^\infty dx \frac{x^5}{x^2 + 1} \left[\frac{1}{e^{\beta\nu x} - 1} - \frac{1}{e^{\beta'\nu x} - 1} \right] \\ &= \frac{\pi}{2\nu} (T' - T) + \frac{1}{2} \ln \frac{T'}{T} + \frac{1}{2} \psi \left(\frac{\nu}{2\pi T'} \right) - \frac{1}{2} \psi \left(\frac{\nu}{2\pi T} \right) - \frac{\pi^2}{6\nu^2} (T^2 - T'^2) + \frac{\pi^4}{15\nu^4} (T^4 - T'^4). \end{aligned} \quad (6.14b)$$

This is plotted in Fig. 10. The values there are to be multiplied by the prefactor in Eq. (6.14a), which for the area of the plate being $S = 1 \text{ cm}$, $t = w = 10 \text{ nm}$, and, appropriate for gold, $\omega_p = 9 \text{ eV}$, $\nu = 0.035 \text{ eV}$, is $\sim 10^{-13} \text{ N}$. Again, this force should be observable.

⁵ For this planar geometry, it might seem more convenient to use a $(2 + 1)$ -dimensional breakup,

$$\Gamma_{ij}(\mathbf{r}, \mathbf{r}'; \omega) = \int \frac{(d\mathbf{k}_\perp)}{(2\pi)^2} e^{i\mathbf{k}_\perp \cdot (\mathbf{r} - \mathbf{r}')_\perp} g_{ij}(z, z'; \mathbf{k}_\perp, \omega). \quad (6.9)$$

Carrying out the trace over the Green's functions, and simplifying to the case that the susceptibility is independent of x and y , we readily obtain

$$I_{AB} = -\frac{S}{32} \int_{|\mathbf{k}_\perp| < |\omega|} \frac{(d\mathbf{k}_\perp)}{(2\pi)^2} \int_A dz \int_B dz' \frac{\lambda^4 + k^4}{\lambda} \sin 2\lambda(z - z') \quad (6.10)$$

Now, if the two sides of the thin plate have small thickness t_A and t_B , respectively, we can expand the sine for small z and z' and find the same result as Eq. (6.11).

VII. FRICTION

Of course, once a body is put in motion by the self-propulsive force, it will experience quantum friction in the vacuum. This friction was considered, in first order, for example, in Ref. [28], but primarily in the condition of nonequilibrium steady state (NESS). The general formula for the formula for the frictional force on a particle in its rest frame is given by Eq. (5.7) there, and shows the effects of field and dipole fluctuations,,

$$F^P = \frac{1}{3\pi^2\gamma v} \int_0^\infty d\omega \omega^4 \operatorname{Im} \alpha_P \int_{\gamma(1-v)}^{\gamma(1+v)} dy (y - \gamma) f_f^P(y) \left(\frac{1}{e^{\beta\omega y} - 1} - \frac{1}{e^{\beta'\omega} - 1} \right), \quad (7.1)$$

where P designates the polarization state of the particle, with the structure functions being $[\gamma = (1 - v^2)^{-1/2}]$

$$f_f^P(y) = \begin{cases} \frac{3}{2\gamma v}, & \text{ISO,} \\ \frac{3}{4\gamma v} \left(1 - \frac{(y-\gamma)^2}{\gamma^2 v^2} \right), & \text{ZZ.} \end{cases} \quad (7.2)$$

Here, the particle is described by a mean polarizability,

$$\alpha(\omega) = \int (d\mathbf{r}) \chi(\mathbf{r}; \omega). \quad (7.3)$$

ISO means a particle which is isotropically polarizable, and ZZ means one which is only polarizable in the z direction, the direction of motion. Due to the symmetry of the y integrand about $y = \gamma$, the second term here, due to dipole fluctuations, vanishes, and hence there is no dependence on the temperature of the particle. (See Appendix A for the second-order correction to the force.)

For a needle moving in the direction of its axis, the ZZ polarization would seem to be appropriate.⁶ When the force for this case is worked out for low velocities, we obtain

$$F_f^{\text{ZZ}} = -\frac{1}{5} \frac{v\beta}{12\pi^2} \int_0^\infty d\omega \omega^5 \operatorname{Im} \alpha(\omega) \frac{1}{\sinh^2 \beta\omega/2}, \quad (7.4)$$

which is just 1/5 the Einstein-Hopf formula for an isotropic particle. The essential point here is that F_f is proportional to the velocity in the low-velocity limit.

Due to the self-propulsive force, the body, out of equilibrium with its environment, will begin to accelerate. It will reach a terminal velocity v_T when the propulsive force exactly balances the frictional force,

$$F_p + v_T F'_f = 0, \quad v_T = -\frac{F_p}{F'_f}. \quad (7.5)$$

Using the same model for the needle as in Sec. III, the derivative of the frictional force is

$$F'_f = -\frac{2C\omega_p^2\nu}{15\pi^2\beta^2} \int_0^\infty dx \frac{x^4}{x^2 + (\beta\nu/2)^2} \frac{1}{\sinh^2 x}, \quad (7.6)$$

where for $\beta = 40$ (eV)⁻¹ (T = room temperature) and a gold needle, $\beta\nu/2 = 0.7$, and we find the x integral here evaluates to 0.90. Then, from the propulsive force (3.10a), we obtain the terminal velocity

$$v_T = -\frac{F_p}{F'_f} = \frac{\chi_A \beta_0^2 \beta^2}{8} \frac{r_0^2}{a_0 a^5} \frac{\hat{F}}{0.90}. \quad (7.7)$$

(The velocity is in the $-z$ direction because $\hat{F} < 0$ if $T' > T$.) For a needle of 1 cm half-length and radius 10 nm, at a temperature twice that of the 300 K background, this equals 7.7×10^{-8} or about 20 m/s. This would be seem to be very observable, if the nonequilibrium temperature imbalance can be maintained.

However, it would take an extraordinarily long time to reach this terminal velocity. From Newton's law,

$$v(t) = v_T \left(1 - e^{-t/t_0} \right), \quad (7.8)$$

⁶ Actually, in this weak-susceptibility approximation the susceptibility is assumed isotropic, so it might be more accurate to multiply the friction by a factor of 5.

where the characteristic time is estimated from above to be

$$t_0 = \frac{m}{F'_f} = \frac{15\pi^2\beta^2\rho}{2\omega_p^2\nu} \frac{1}{0.9}. \quad (7.9)$$

where ρ is the density of the metal part of the needle. Putting in numbers appropriate for gold, we find something like $t_0 \sim 2.7 \times 10^9$ s, about 80 years. This long time is a reflection of the weakness of the frictional force.

VIII. RELAXATION TO THERMAL EQUILIBRIUM

Quantum friction appears then to play a negligible role. However, unless the body is equipped with a mechanism to maintain its elevated temperature, like a real quantum thruster [46], it will rapidly cool to the temperature of the environment. We estimate this effect as in Ref. [42]: The rate of heat loss

$$\frac{dQ}{dt} = C_V(T') \frac{dT'}{dt} = P(T', T), \quad (8.1)$$

where $C_V(T')$ is the specific heat of the body at temperature T' , and the power for a slowly moving body is given by Eq. (6.3) [28], or its generalization (see Appendix B)

$$P(T', T) = \frac{1}{3\pi^2} \int_0^\infty d\omega \omega^4 \operatorname{Im} \operatorname{tr} \alpha(\omega) \left[\frac{1}{e^{\beta\omega} - 1} - \frac{1}{e^{\beta'\omega} - 1} \right], \quad (8.2)$$

but this transcends the weak susceptibility limit, in that the polarizability is not simply $\alpha(\omega) = \int(d\mathbf{r})\chi(\mathbf{r}, \omega)$. Then, the time to cool the body from temperature T'_0 to temperature T'_1 is

$$t_1 = \int_{T'_0}^{T'_1} dT' \frac{C_V(T')}{P(T', T)}. \quad (8.3)$$

We can solve this equation (numerically) for $T'_1(t_1, T)$ (assuming fixed environmental temperature), and then find the body's acceleration in terms of the propulsive force at that time (m is the mass of the body),

$$m \frac{dv(t)}{dt} = F_p(T'(t), T), \quad (8.4)$$

which, when integrated over all time, gives the terminal velocity,

$$v_T = \frac{1}{m} \int_0^\infty dt F_p(T'(t), T). \quad (8.5)$$

This is precisely the scheme advocated in Ref. [44].

Let us specifically consider the example of the Janus ball discussed in Sec. V. For the cooling, we consider the high-temperature approximation of the Debye model treated in Ref. [42], together with the Lorenz-Lorentz model for the polarizability, which gives

$$t = t_c \int_{T'_0/T}^{T'/T} du \frac{1}{1 - u^6}, \quad t_c = \frac{21}{8\pi^4} \frac{n\omega_p^2}{\nu T^5}, \quad (8.6)$$

n being the number density. The time scale t_c for gold at room temperature is about 2,000 s. The numerical inverse function $T'(t)$ is shown in Fig. 11. Now we insert this into the force formula for the propulsive force on a small Janus ball, given by Eq. (5.7). Then we use the expression for the terminal velocity (8.5) to give

$$v_T = \lim_{t \rightarrow \infty} v(t), \quad v(t) = \frac{7}{72\pi^5} \chi_A \omega_p^4 \frac{n}{m} \frac{\nu^6 a^7}{T^5} \int_0^{t/t_c} d\tau \hat{F}(\tau), \quad \tau = \frac{t}{t_c}. \quad (8.7)$$

The prefactor here, for the metallic half-ball being gold, having a radius 100 nm, in a vacuum environment at room temperature, is about $20\chi_A \mu\text{m/s}$. The dimensionless force, $\hat{F}(t/t_c)$ is shown in Fig. 12. The numerical integral of \hat{F} for large t/t_0 when $T'_0/T = 2$ gives about -15 , yielding roughly $v_T = -300 \mu\text{m/s}$, the asymptotic value being achieved by about $0.1 t_c \approx 200$ s. If there had been no thermal cooling, in this time the body would have reached a velocity of about 0.1 cm/s . Increasing the initial temperature of the particle to $T'_0 = 10T$ increases the terminal velocity by about a factor of 6, while reducing the time to reach equilibrium by about four orders of magnitude. (The discussion in this paragraph assumes that the thermal radiation from the metal portion dominates the energy loss mechanism, which is true, at least perturbatively.)

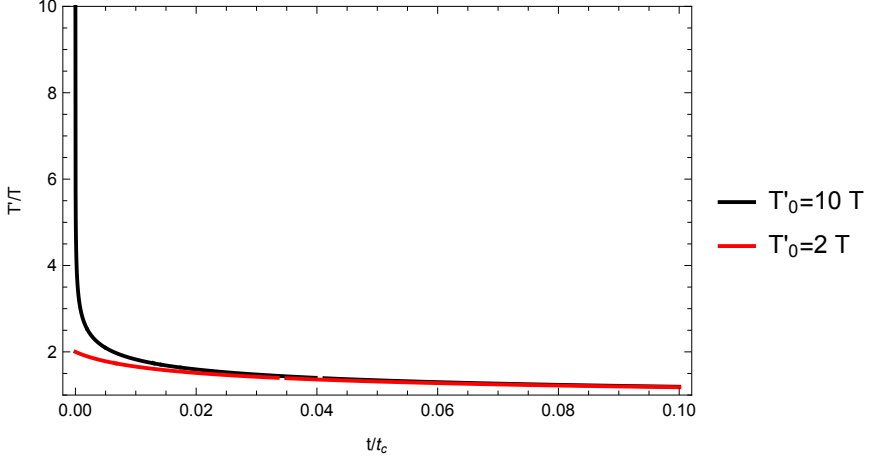


FIG. 11. The temperature T' of the body (relative to that of the environment T) in terms of the cooling time relative to the scale t_c . The two curves are for an initial temperature ratio of 10 (upper) and 2 (lower).

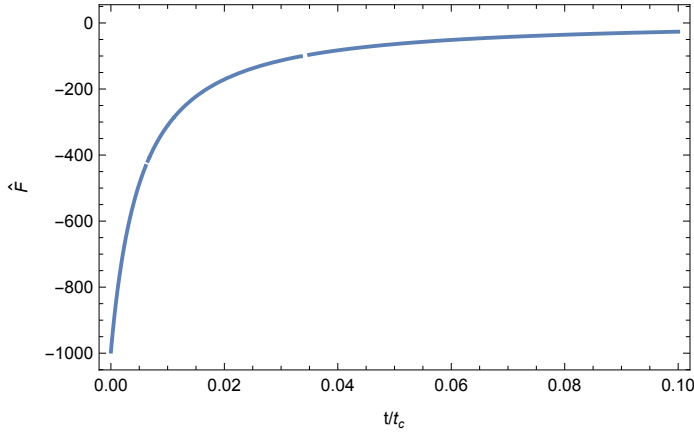


FIG. 12. The dimensionless force \hat{F} for a Janus ball, the metallic half of which is gold, as a function of the time t/t_c , at a vacuum temperature of $T = 300$ K, and an initial temperature of the nanoball of $T'_0 = 600$ K.

A. Weak-susceptibility model

The above treatment might seem inconsistent, since the perturbative susceptibility is used for the propulsion but the dressed Lorenz-Lorentz polarizability is used for the cooling. If, instead, we use the weak-coupling susceptibility for the metal,

$$\text{Im } \chi(\omega) = \frac{\omega_p^2 \nu}{\omega(\omega^2 + \nu^2)}, \quad (8.8)$$

we obtain instead of Eq. (8.6) the time to cool from T'_0 to T'_1

$$t_1 = -\frac{6\pi^2 n}{\nu^2 \omega_p^2} \int_{\beta'_1 \nu}^{\beta'_1 \nu} \frac{dx'}{x'^2} \left[\ln \frac{x'}{x} + \psi\left(\frac{x}{2\pi}\right) - \psi\left(\frac{x'}{2\pi}\right) + \pi \left(\frac{1}{x} - \frac{1}{x'} \right) + \frac{\pi^2}{3} \left(\frac{1}{x^2} - \frac{1}{x'^2} \right) \right]^{-1}. \quad (8.9)$$

The prefactor here, t_c , for gold is about 2×10^{-4} s. This is then inverted to find T'/T as a function of $\tau = t'/t_c$ as above. Then the terminal velocity for a Janus ball, half of which is gold, is found from Eq. (8.5) to be

$$v_T = \frac{1}{3} \frac{\chi_A \nu^5 a^4}{m_{\text{Au}}} \int_0^\infty d\tau \hat{F}(T'(\tau), T), \quad (8.10)$$

m_{Au} being the mass of a gold atom, where the prefactor is only 5×10^{-1} nm/s, while the integral is only about 100, so this is ridiculously small.⁷

One might think one could boost this substantially by considering a macroscopic object. But, presumably it should be thin so that thicknesses do not exceed the skin depth, otherwise the weak susceptibility approach to the force will not be valid. So let's consider the thin spherical shell model of Sec. IV for which the propulsive force is given, approximately, by Eq. (4.7). Since the cooling time is independent of the shape of the body, we can use Eq. (8.9), and then find the terminal velocity from

$$v_T = \frac{3}{16\pi} \frac{|\mathcal{N}| \nu t}{m_{\text{Au}} a} \chi_A \int_0^\infty d\tau |\hat{F}(T'(\tau), T)| \quad (8.11)$$

The prefactor evaluates to $2 \times 10^{-10} \chi_A$ m/s, where the integral over Eq. (4.7b) is about 0.4, so this still remains beyond experimental reach.

IX. CONCLUSIONS

In this paper we have tried to give a systematic treatment of self-propulsion of an inhomogeneous body in vacuum, which occurs not in first order, but in second order in the susceptibility (or polarizability) of the body. For a force to occur, the body must have nonuniform electric susceptibility, be dissipative, and be out of thermal equilibrium with the background. For a body hotter than the vacuum environment and having two different halves, the force is in the direction of the side having the lowest emissivity, the radiation emitted being predominantly from the opposite side. We consider four different configurations: a thin needle, a thin spherical shell, a solid nanoball, and finally a thin plate. Except in the last case, one side is regarded as non-dissipative, while the other is modeled as a Drude metal; for the thin plate, the nonmetal side is modelled as a total blackbody absorber. Presumably, in all cases, the objects must have small thicknesses, so that the skin depth is larger than the thickness.⁸ Therefore, the forces must be very small (not sufficient for a quantum thruster [46]), but probably amenable to observation if the temperature imbalance could be maintained. Quantum vacuum friction will eventually cause the particle to acquire a terminal velocity. But if the system is allowed to relax to thermal equilibrium, the body might reach an observable velocity in a matter of seconds; however, this conclusion sensitively depends on the model of heat loss.

ACKNOWLEDGMENTS

This work was supported in part by the US National Science Foundation, grant number 2008417. GK thanks the Homer L. Dodge Department of Physics and Astronomy at the University of Oklahoma for its hospitality. We thank Xin Guo, Prachi Parashar, and Steve Fulling for collaborative assistance. This paper reflects solely the authors' personal opinions and does not represent the opinions of the authors' employers, present and past, in any way. For the purpose of open access, the authors have applied a CCBY public copyright license to any Author Accepted Manuscript version arising from this submission.

Appendix A: Force on moving body

In this appendix we derive the force on a body moving with velocity \mathbf{v} in the z direction, which in general will include both a propulsive force and a frictional force. For simplicity of presentation, we will restrict attention to the case when the susceptibility has only a nonzero zz component, because that greatly simplifies the form of the Lorentz boosts. We will work in a $(3+1)$ -dimensional wave-vector representation. Starting from Eq. (2.1), we have for the force on the dielectric body in its rest frame

$$F_z = \int (d\mathbf{r}) \int \frac{d\omega d\nu}{(2\pi)^2} \int \frac{(d\mathbf{k})}{(2\pi)^3} \frac{(d\mathbf{q})}{(2\pi)^3} e^{-i(\omega+\nu)t} e^{i(\mathbf{k}+\mathbf{q}) \cdot \mathbf{r}} \mathbf{P}(\mathbf{k}, \omega) i q_z \mathbf{E}(\mathbf{q}, \nu), \quad (A1)$$

where all quantities are in the rest frame of the body. Here, we have omitted the first term in Eq. (2.1), because it will always vanish.

⁷ Note that the ratio of the t_c scales in Eqs. (8.6) and (8.9) is $\frac{7}{16\pi^6} \frac{\omega_p^4 \nu}{T^5} \sim 10^7$, which is also the ratio of the forces, apart from the dimensionless integrals, which are in the ratio of 15/100.

⁸ This may also validate the weak-susceptibility approximation, in that we take the polarizability to be simply the volume integral of the susceptibility.

1. First-order friction

To begin, we examine this in first order, where in place of Eqs. (2.3) we have in momentum space (leaving off the component indices, which are always z in our case)

$$P(\mathbf{k}, \omega) = \int \frac{d\mathbf{k}'}{(2\pi)^3} \chi(\mathbf{k} - \mathbf{k}') E(\mathbf{k}', \omega), \quad (\text{A2a})$$

$$\tilde{E}(\mathbf{k}, \omega) = \Gamma(\mathbf{k}, \omega) \tilde{P}(\mathbf{k}, \omega). \quad (\text{A2b})$$

(Quantities without tildes are in the rest frame of the body, while those with tildes are in the rest frame of the radiation.) Expanding P to first order in E , we have

$$F_z^{(1,0)} = \int \frac{d\omega}{2\pi} \frac{d\nu}{2\pi} \frac{(d\mathbf{k})}{(2\pi)^3} \frac{(d\mathbf{k}')}{(2\pi)^3} e^{-i(\omega+\nu)t} (-ik_z) \chi(\mathbf{k} - \mathbf{k}', \omega) E(\mathbf{k}', \omega) E(-\mathbf{k}, \nu), \quad (\text{A3})$$

where the body rest frame value of the electric field, E is related to that in the radiation rest frame, \tilde{E} , by

$$E(\mathbf{k}, \omega) = \tilde{E}(\tilde{\mathbf{k}}, \tilde{\omega}), \quad (\text{A4})$$

(this is where the simplification to have only z polarization is crucial). The boosted momentum and frequency variables are

$$\tilde{k}_z = \gamma(k_z + \omega v), \quad \tilde{k}_{x,y} = k_{x,y}, \quad \tilde{\omega} = \gamma(\omega + k_z v), \quad (\text{A5})$$

in terms of the relativistic dilation factor $\gamma = (1 - v^2)^{-1/2}$. Then, we use the FDT in the form

$$\langle \mathcal{S} \tilde{E}(\tilde{\mathbf{k}}, \tilde{\omega}) \tilde{E}(\tilde{\mathbf{q}}, \tilde{\nu}) \rangle = (2\pi)^4 \delta(\tilde{\omega} + \tilde{\nu}) \delta(\tilde{\mathbf{k}} + \tilde{\mathbf{q}}) \text{Im} \Gamma(\tilde{\mathbf{k}}, \tilde{\omega}) \coth \frac{\beta \tilde{\omega}}{2}. \quad (\text{A6})$$

The product of δ functions is invariant under a Lorentz boost,

$$\delta(\tilde{\omega} + \tilde{\nu}) \delta(\tilde{\mathbf{k}} + \tilde{\mathbf{q}}) = \delta(\omega + \nu) \delta(\mathbf{k} + \mathbf{q}), \quad (\text{A7})$$

as is the zz component of the vacuum Green's dyadic:

$$\tilde{\Gamma}(\tilde{\mathbf{k}}, \tilde{\omega}) = \Gamma(\mathbf{k}, \omega) = \frac{k_\perp^2}{k^2 - (\omega + i\epsilon)^2}. \quad (\text{A8})$$

The imaginary part of the latter is

$$\text{Im} \Gamma(\mathbf{k}, \omega) = k_\perp^2 \pi \text{sgn}(\omega) \delta(k^2 - \omega^2). \quad (\text{A9})$$

Putting this into the formula for the force (A3) we obtain

$$\begin{aligned} F_z^{(1,0)} &= \int \frac{d\omega (d\mathbf{k})}{(2\pi)^4} (-ik_z) \chi(\mathbf{0}, \omega) \text{Im} \Gamma(\mathbf{k}, \omega) \coth \frac{\beta \tilde{\omega}}{2} \\ &= \frac{1}{(2\pi)^2} \int_0^\infty d\omega \int_{-\omega}^\omega dk_z \text{Im} \chi(\mathbf{0}, \omega) k_x (\omega^2 - k_z^2) \frac{1}{e^{\beta \gamma(\omega + k_z v)} - 1}. \end{aligned} \quad (\text{A10})$$

Introducing the variable y through $\gamma(\omega + k_z v) = \omega y$, we obtain exactly the result (7.1) for the ZZ polarization: there is no contribution at $v = 0$ and the PP or the $(0,1)$ contribution is zero, because the corresponding integral is odd in k_z .

2. Second-order force and friction

To obtain a propulsive force, we have to go to second order in the susceptibility. We begin by expanding the free energy so that P is expanded once, and E is expanded twice, the term we refer to as (1,2). For simplicity of notation, we leave off integration elements:

$$P(\mathbf{k}, \omega) E(\mathbf{k}', \nu) = \chi(\mathbf{k} - \mathbf{k}'', \omega) \tilde{E}(\tilde{\mathbf{k}}'', \tilde{\omega}) \Gamma(\tilde{\mathbf{k}}', \tilde{\nu}) \chi(\mathbf{k}' - \mathbf{k}''', \nu) \tilde{E}(\tilde{\mathbf{k}}''', \tilde{\nu}), \quad (\text{A11})$$

doing successive Lorentz boosts back and forth between the two natural frames, and then use the FDT (A6). The result for this force component is

$$F_z^{(1,2)} = \int \frac{d\omega (d\mathbf{k}) (d\mathbf{k}')}{(2\pi)^7} k'_z |\chi(\mathbf{k} - \mathbf{k}', \omega)|^2 \text{Im} \Gamma(\mathbf{k}, \omega) \text{Im} \Gamma(\mathbf{k}', \omega) \coth \frac{\beta \tilde{\omega}}{2}, \quad (\text{A12})$$

where the second imaginary part of a Green's dyadic comes from the symmetry $(\omega, \mathbf{k}, \mathbf{k}') \rightarrow -(\omega, \mathbf{k}, \mathbf{k}')$, and we have noted that

$$\chi(\mathbf{k}, \omega)^* = \chi(-\mathbf{k}, -\omega), \quad (\text{A13})$$

because the underlying coordinate-space response function is real.

Following the same procedure, expanding P out to third order, we find

$$F_z^{(3,0)} = \int \frac{d\omega (d\mathbf{k}) (d\mathbf{k}')}{(2\pi)^7} (-ik_z) \chi(\mathbf{k} - \mathbf{k}', \omega) \chi(\mathbf{k}' - \mathbf{k}, \omega) \Gamma(\mathbf{k}', \omega) \text{Im} \Gamma(\mathbf{k}, \omega) \coth \frac{\beta \tilde{\omega}}{2}. \quad (\text{A14})$$

The two contributions to the EE force correspond to what we called I [Eq. (A14)] and II [Eq. (A12)] in Ref. [27]. We note that the (3,0) contribution vanishes at $v = 0$ because it is then antisymmetric under the reflection $(\mathbf{k}, \mathbf{k}') \rightarrow -(\mathbf{k}, \mathbf{k}')$. It is possible then to show that the $v = 0$ contribution of $F^{(1,2)}$ coincides with that found from Eq. (2.6a). namely,

$$F_z^{\text{EE}} \Big|_{v=0} = \int (d\mathbf{r})(d\mathbf{r}') \frac{d\omega}{2\pi} \text{Im}[\chi(\mathbf{r}; \omega) \chi(\mathbf{r}'; \omega)^*] \text{Im} \Gamma(\mathbf{r}, \mathbf{r}'; \omega) \nabla_z \text{Im} \Gamma(\mathbf{r}, \mathbf{r}'; \omega) \coth \frac{\beta \omega}{2}, \quad (\text{A15})$$

having the same form as Eq. (2.9).

In general, however, because the product of susceptibilities in $F_z^{(3,0)}$ is not real, the real part of $\Gamma(\mathbf{k}', \omega)$ occurs, which leads to divergences when the integration over \mathbf{k}' is performed. The solution to this difficulty was provided in Ref. [27]: when $F_z^{(1,0)}$ [Eq. (A10)] and $F_z^{(3,0)}$ [Eq. (A14)] are combined, we have

$$F_z^{(1,0)+(3,0)} = \int \frac{d\omega (d\mathbf{k}) (d\mathbf{k}')}{(2\pi)^7} (-ik_z) \hat{\chi}(\mathbf{k} - \mathbf{k}', \omega) \text{Im} \Gamma(\mathbf{k}, \omega) \coth \frac{\beta \tilde{\omega}}{2}, \quad (\text{A16})$$

where

$$\hat{\chi}(\mathbf{k} - \mathbf{k}', \omega) = \chi(\mathbf{k} - \mathbf{k}', \omega) [(2\pi)^3 \delta(\mathbf{k} - \mathbf{k}') + \Gamma(\mathbf{k}', \omega) \chi(\mathbf{k}' - \mathbf{k}, \omega)]. \quad (\text{A17})$$

These are the first two terms of an infinite series, written in symbolic notation:

$$\hat{\chi} = \chi_0 (1 - \Gamma \chi_0)^{-1}, \quad (\text{A18})$$

where we have denoted by χ_0 , the bare intrinsic susceptibility, what we previously called χ . Then, breaking up Γ into its real and imaginary parts, we have for the effective susceptibility, just as in Eq. (4.31) of Ref. [27],

$$\hat{\chi} = \chi (1 - i \text{Im} \Gamma \chi)^{-1}, \quad (\text{A19a})$$

in terms of the renormalized intrinsic susceptibility

$$\chi = \chi_0 (1 - \text{Re} \Gamma \chi_0)^{-1}. \quad (\text{A19b})$$

This is how the bare intrinsic susceptibility is dressed by the radiation field. (After all, the momentum-space Fourier transform of χ is the generalization of the polarizability discussed in Ref. [27].) Therefore, we conclude that the renormalized version of $F^{(3,0)}$ should read

$$F_{z,R}^{(3,0)} = \int \frac{d\omega (d\mathbf{k}) (d\mathbf{k}')}{(2\pi)^7} k_z \text{Re}[\chi(\mathbf{k} - \mathbf{k}', \omega) \chi(\mathbf{k}' - \mathbf{k}, \omega)] \text{Im} \Gamma(\mathbf{k}', \omega) \text{Im} \Gamma(\mathbf{k}, \omega) \coth \frac{\beta \tilde{\omega}}{2}, \quad (\text{A20})$$

which is free of all difficulties.

For the PP fluctuation contributions, the calculation proceeds similarly. Now we either expand the free energy out to third order in E , giving a (0,3) contribution, or expand P out to second order and E out to first, the (2,1) term. The FDT (2.4b), in the Fourier domain, reads

$$\langle \mathcal{S} P(\mathbf{k}, \omega) P(\mathbf{k}', \nu) \rangle = 2\pi \delta(\omega + \nu) \Im \chi(\mathbf{k} + \mathbf{k}', \omega) \coth \frac{\beta' \omega}{2}, \quad (\text{A21a})$$

with

$$\Im\chi(\mathbf{k} + \mathbf{k}', \omega) = \frac{1}{2i} [\chi(\mathbf{k} + \mathbf{k}', \omega) - \chi(\mathbf{k} + \mathbf{k}', -\omega)], \quad (\text{A21b})$$

neither the imaginary nor the anti-Hermitian part. The two contributions to the force are, respectively,⁹

$$F_z^{(0,3)} = i \int \frac{d\omega(d\mathbf{k})(d\mathbf{k}')}{(2\pi)^7} k_z \Gamma(\mathbf{k}, -\omega) \Gamma(\mathbf{k}', -\omega) \chi(\mathbf{k} - \mathbf{k}', -\omega) \Im\chi(\mathbf{k}' - \mathbf{k}, -\omega) \coth \frac{\beta' \omega}{2}, \quad (\text{A22a})$$

$$F_z^{(2,1)} = -i \int \frac{d\omega(d\mathbf{k})(d\mathbf{k}')}{(2\pi)^7} k_z \Gamma(\mathbf{k}, -\omega) \Gamma(\mathbf{k}', \omega) \chi(\mathbf{k} - \mathbf{k}', \omega) \Im\chi(\mathbf{k}' - \mathbf{k}, \omega) \coth \frac{\beta' \omega}{2}. \quad (\text{A22b})$$

Using the symmetries $(\mathbf{k}, \mathbf{k}') \rightarrow -(\mathbf{k}, \mathbf{k}')$ and $\mathbf{k} \leftrightarrow \mathbf{k}'$, we obtain the total PP contribution to the force

$$F^{(0,3)+(2,1)} = -\frac{1}{4} \int \frac{d\omega(d\mathbf{k})(d\mathbf{k}')}{(2\pi)^7} (k_z - k'_z) \text{Im}\Gamma(\mathbf{k}, \omega) \text{Im}\Gamma(\mathbf{k}', \omega) [|\chi(\mathbf{k}' - \mathbf{k}, \omega)|^2 - |\chi(\mathbf{k} - \mathbf{k}', \omega)|^2] \coth \frac{\beta' \omega}{2}. \quad (\text{A23})$$

and the total $v = 0$ propulsive force is

$$\begin{aligned} F^{EE+PP} = & - \int_0^\infty \frac{d\omega}{2\pi} \int \frac{(d\mathbf{k})(d\mathbf{k}')}{(2\pi)^6} (k_z - k'_z) \text{Im}\Gamma(\mathbf{k}, \omega) \text{Im}\Gamma(\mathbf{k}', \omega) [|\chi(\mathbf{k} - \mathbf{k}', \omega)|^2 - |\chi(\mathbf{k}' - \mathbf{k}, \omega)|^2] \\ & \times \left[\frac{1}{e^{\beta\omega} - 1} - \frac{1}{e^{\beta'\omega} - 1} \right]. \end{aligned} \quad (\text{A24})$$

This agrees with the propulsive force given in Sec. II.

As for the $v \neq 0$ frictional force, we can compare with the second-order results of Ref. [27], where we considered a point particle with a real polarizability. Then there are only EE fluctuations, and the spatial Fourier transform of the susceptibility is the polarizability of the particle, $\chi(\mathbf{k} - \mathbf{k}', \omega) = \alpha(\omega)$. Then it is straightforward to show that the EE force is entirely frictional and coincides with Eq. (3.16) of Ref. [27]. This is because

$$\int dk_x \text{Im}\Gamma(\mathbf{k}, \omega) = \int dk_x (k_x^2 + k_y^2) \text{Im} \frac{1}{k_x^2 + k_y^2 + k_z^2 - (\omega - i\epsilon)^2} = \pi \text{sgn}(\omega) \frac{\omega^2 - k_z^2}{\sqrt{\omega^2 - k_y^2 - k_z^2}} \eta(\omega^2 - k_y^2 - k_z^2). \quad (\text{A25})$$

That is, the frictional force in this case is

$$F^{(3,0)+(1,2)} = \frac{1}{32\pi^3} \int_0^\infty d\omega \int_0^\omega dk_z \int_0^\omega dk'_z \alpha^2(\omega) (k_z - k'_z) (\omega^2 - k_z^2) (\omega^2 - k_z'^2) \frac{1}{e^{\beta\gamma(\omega+k_z v)} - 1}. \quad (\text{A26})$$

If $F^{(1,2)}$ is expanded to first order in v , the frictional force so arising, proportional to $k_z k'_z$, vanishes by $k_z \leftrightarrow k'_z$ symmetry. This statement is true for any object with uniform susceptibility; that is, the frictional force only arises from $F^{(3,0)}$, while the propulsive force on a nonuniform object has an EE contribution coming only from $F^{(1,2)}$. (We already recognized the latter in Sec. II, while the former was observed in Ref. [27].) For a small object, with polarizability proportional to its volume, this second-order friction would be expected to be much smaller than the first-order friction given in Eq. (7.1). Consider the thin needle as an example. The friction comes only from $F^{(3,0)}$, and, in the approximation that the friction arises from a region where the susceptibility is real and uniform, reads, for low velocity (the Einstein-Hopf limit),

$$F = 16C^2 v T^6 \int_0^\infty dz z^6 \chi(2Tz)^2 \frac{r(zT)}{\sinh^2 z}, \quad (\text{A27})$$

where

$$r(t) = \int_0^1 dx \int_0^1 dy \frac{x^2(1-x^2)(1-y^2)}{(x-y)^2} \sin^2[(x-y)t]. \quad (\text{A28})$$

The integral $r(t)$ may be given in closed form in terms of the sine-integral function, but only the large- t behavior is relevant for a 1 cm object at room temperature because typical values of t are of order $bT = 625$ at room temperature:

$$r(t) \sim \frac{8\pi t}{105}, \quad t \gg 1. \quad (\text{A29})$$

For a representative value of susceptibility χ_0 , the force (A27) is smaller than the frictional force found in Eq. (7.1) by a factor of $5 \times 10^{-7} \chi_0^2$.

⁹ Note that no renormalization of $F_z^{(0,3)}$ is necessary, because $F_z^{(0,1)}$ vanishes.

Appendix B: Radiated energy

In Ref. [28] we derived the energy lost by a polarizable particle out of thermal equilibrium by looking at the rate with which the particle does work on the field. Alternatively, we can examine the rate at which the energy flows across a surface surrounding a body, which follows from energy conservation,

$$\frac{\partial}{\partial t}u + \nabla \cdot \mathbf{S} + \mathbf{j} \cdot \mathbf{E} = 0, \quad (\text{B1})$$

provided, as is the case here, that the situation is stationary. Here the energy flux vector or Poynting vector is

$$\mathbf{S}(\mathbf{r}, t) = \int \frac{d\omega}{2\pi} \frac{d\nu}{2\pi} e^{-i(\omega+\nu)t} \mathbf{E}(\mathbf{r}; \omega) \times \left[\frac{1}{i\nu} \nabla \times \mathbf{E}(\mathbf{r}; \nu) \right]. \quad (\text{B2})$$

If the electric field is expanded out to first order with the polarization as given in Eq. (2.3a), and we use the FDT (2.4b) for the polarization field product, we find for the PP fluctuation part of the Poynting vector

$$S_k^{\text{PP}}(\mathbf{r}) = - \int (d\mathbf{r}') \frac{d\omega}{2\pi} \frac{1}{i\omega} \Gamma_{ij}(\mathbf{r} - \mathbf{r}'; \omega) \text{Im} \chi_{jl}(\mathbf{r}'; \omega) \coth \frac{\beta' \omega}{2} [\nabla_k \Gamma_{il}(\mathbf{r} - \mathbf{r}'; -\omega) - \nabla_i \Gamma_{kl}(\mathbf{r} - \mathbf{r}'; -\omega)]. \quad (\text{B3})$$

Now we imagine surrounding the body with a sphere of radius R , large compared to the size of the body and centered on it. Then the Green's dyadic appearing here is asymptotically

$$\Gamma_{ij}(\mathbf{R}; \omega) \sim \omega^2 (\mathbf{1} - \hat{\mathbf{R}} \hat{\mathbf{R}}) \frac{e^{i\omega R}}{4\pi R}, \quad R \gg a, \quad (\text{B4})$$

where a is a typical size of the object. The corresponding expectation value of the flux vector is

$$S_k^{\text{PP}}(\mathbf{r}) = \int \frac{d\omega}{2\pi} (d\mathbf{r}') \frac{\omega^4}{(4\pi R)^2} \hat{R}_k (\delta_{ij} - \hat{R}_i \hat{R}_j) \text{Im} \chi_{ij}(\mathbf{r}'; \omega) \coth \frac{\beta' \omega}{2} \quad (\text{B5a})$$

$$\rightarrow 2 \int \frac{d\omega}{2\pi} (d\mathbf{r}') \frac{\omega^4}{(4\pi R)^2} \hat{R}_k \text{Im} \chi(\mathbf{r}'; \omega) \coth \frac{\beta' \omega}{2}, \quad (\text{B5b})$$

where the second form applies for isotropic susceptibility. Integrating this over a large sphere surrounding the body gives the total energy emitted per unit time:

$$\int d\sigma \hat{\mathbf{R}} \cdot \mathbf{S}^{\text{PP}}(\mathbf{r}) = \frac{1}{4\pi^2} \int d\omega \omega^4 \text{Im} \alpha(\omega) \coth \frac{\beta' \omega}{2}. \quad (\text{B6})$$

Here, we use the lowest-order susceptibility, $\alpha(\omega) = \int (d\mathbf{r}') \chi(\mathbf{r}'; \omega)$.

What we did in the preceding paragraph is what we denote as the (1,1) term in the expansion. To obtain the EE fluctuation contribution, we compute, in the same way, the (2,0) and (0,2) expansions. The result is as expected; the total flux vector for large R being for arbitrary polarizability

$$S_k = S_k^{\text{PP}} + S_k^{\text{EE}} = \frac{\hat{R}_k}{(4\pi R)^2} \int \frac{d\omega}{2\pi} \omega^4 (\delta_{ij} - \hat{R}_i \hat{R}_j) \text{Im} \alpha_{ij}(\omega) \left(\coth \frac{\beta' \omega}{2} - \coth \frac{\beta \omega}{2} \right). \quad (\text{B7})$$

Appendix C: Dielectric in front of a mirror

To understand the sense of the force, which in all the examples we have considered is in the direction of the metal side of the composite object, we consider a simple example of a perfectly conducting plane, a perfect mirror, located at $z = 0$, attached to which is a dilute dielectric body, as shown in Fig. 13. It is evident from the diagram that, because energy is radiated to the right by the composite assembly, there will be a force on that assembly to the left, in the $-z$ direction. The purpose of this appendix is to make that picture quantitative.

We treat the effect of the dielectric perturbatively, to first order in its susceptibility, $\chi(\mathbf{r}'; \omega)$. The effect of the mirror is to replace the free electromagnetic Green's dyadic $\mathbf{\Gamma}^{(0)}(\mathbf{r} - \mathbf{r}'; \omega)$ by the Green's dyadic [48]

$$\mathbf{\Gamma}(\mathbf{r}, \mathbf{r}'; \omega) = \mathbf{\Gamma}^{(0)}(\mathbf{r} - \mathbf{r}'; \omega) - \mathbf{\Gamma}^{(0)}(\mathbf{r} - \mathbf{r}' + 2z' \hat{\mathbf{z}}; \omega) \cdot (\mathbf{1} - 2\hat{\mathbf{z}}\hat{\mathbf{z}}), \quad (\text{C1})$$

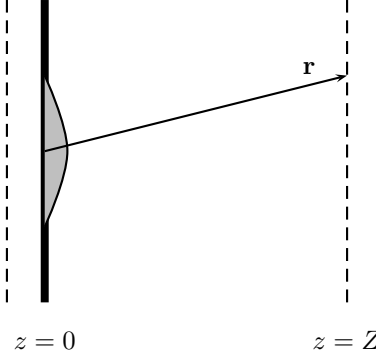


FIG. 13. Perfectly reflecting mirror located in the plane $z = 0$ to which a dilute dielectric is attached. The radiation fields are observed on the distant screen at $z = Z$. The screen to the left of the mirror sees nothing but the background field modified by the mirror. The dielectric is at temperature T' while the background has temperature T .

which has an obvious interpretation in terms of an image charge. We are interested in fields far from the mirror/dielectric assembly, $r \gg r'$, where \mathbf{r}' locates a point within the dielectric. In the radiation zone, then,

$$\mathbf{\Gamma}(\mathbf{r}, \mathbf{r}'; \omega) \sim 2\mathbf{\Gamma}^{(0)}(\mathbf{r}; \omega) \cdot \hat{\mathbf{z}}\hat{\mathbf{z}}. \quad (\text{C2})$$

For large r , the only surviving components of the Green's dyadic are from Eq. (2.12),

$$\Gamma_{xz} \sim -\frac{2\omega^2}{4\pi r} \frac{xz}{r^2} e^{i\omega r}, \quad \Gamma_{yz} \sim -\frac{2\omega^2}{4\pi r} \frac{yz}{r^2} e^{i\omega r} \quad \Gamma_{xz} \sim \frac{2\omega^2}{4\pi r} \left(1 - \frac{z^2}{r^2}\right) e^{i\omega r}. \quad (\text{C3})$$

Now we calculate the first-order energy flux as in Appendix B, see Eq. (B3):

$$S_z = \int \frac{d\omega}{2\pi} (d\mathbf{r}') \frac{1}{\omega} \text{Im} \chi(\mathbf{r}'; \omega) \left(\coth \frac{\beta\omega}{2} - \coth \frac{\beta'\omega}{2} \right) \text{Im} \{ \Gamma_{ij}(\mathbf{r}, \mathbf{r}'; \omega) [\partial_z \Gamma_{ij}(\mathbf{r}, \mathbf{r}'; -\omega) - \partial_i \Gamma_{zj}(\mathbf{r}, \mathbf{r}'; -\omega)] \}, \quad (\text{C4})$$

for isotropic polarizability. When the asymptotic forms of the Green's dyadic are inserted into this, we find

$$S_z \sim -\frac{1}{4\pi^2} \frac{z(r^2 - z^2)}{r^5} \int \frac{d\omega}{2\pi} \omega^4 \text{Im} \alpha(\omega) \left(\coth \frac{\beta\omega}{2} - \coth \frac{\beta'\omega}{2} \right). \quad (\text{C5})$$

Here we have introduced again $\alpha(\omega) = \int (d\mathbf{r}') \chi(\mathbf{r}'; \omega)$. Now we integrate S_z over the infinite screen at $z = Z$ by introducing polar coordinates on that plane:

$$r = Z \sec \theta, \quad \rho = \sqrt{x^2 + y^2} = Z \tan \theta. \quad (\text{C6})$$

Therefore, the total power radiated is

$$P = -\frac{2}{3\pi^2} \int_0^\infty d\omega \omega^4 \text{Im} \alpha(\omega) \left(\frac{1}{e^{\beta\omega} - 1} - \frac{1}{e^{\beta'\omega} - 1} \right). \quad (\text{C7})$$

The sign means that, if $T' > T$, the energy flux is, as is obvious, in the $+z$ direction.

For the force of the composite mirror/dielectric object, we compute the surface integral of the zz component of the electromagnetic stress tensor, T_{zz} , over the same surface, as follows from the local statement of momentum conservation,

$$\frac{\partial}{\partial t} \mathbf{G} + \nabla \cdot \mathbf{T} + \mathbf{f} = \mathbf{0}, \quad (\text{C8})$$

where \mathbf{f} is the force density on all the free and bound charges, \mathbf{T} is the stress tensor, and \mathbf{G} is the momentum density of the field. [The contributions to S_z and T_{zz} from the mirror alone in vacuum is zero.] The force is, in our static situation,

$$F_z = - \int_{z=Z} d\sigma T_{zz} = -\frac{1}{2} \int_{z=Z} d\sigma (E_x^2 + E_y^2 - E_z^2 + H_x^2 + H_y^2 - H_z^2). \quad (\text{C9})$$

The FDT gives PP contributions [that we referred to as (1,1) expansion terms] and EE contributions [(2,0) and (0,2) contributions]. A straightforward calculation for the former leads to the following radiation-zone result:

$$F_z^{\text{PP}} = -2 \int_{z=Z} d\sigma \frac{z^2(x^2 + y^2)}{r^6} \int \frac{d\omega}{2\pi} \text{Im } \alpha(\omega) \frac{\omega^4}{4\pi^2} \coth \frac{\beta'\omega}{2}, \quad (\text{C10})$$

which exhibits the same positional dependence on the screen as the energy flux. The corresponding calculation for the EE contributions involves recognizing the average

$$\text{Im } (e^{i\omega R}) e^{-i\omega R} \rightarrow -\frac{i}{2}, \quad \text{Im } (i e^{i\omega R}) i e^{i\omega R} \rightarrow +\frac{i}{2}; \quad (\text{C11})$$

the result of including the EE and PP contributions is

$$F_z = \frac{1}{8\pi^2} \int_0^\infty d\omega \omega^4 \text{Im } \alpha(\omega) \left(\coth \frac{\beta\omega}{2} - \coth \frac{\beta'\omega}{2} \right). \quad (\text{C12})$$

Indeed, the force is directed in the $-z$ direction, but the precise connection between the energy radiated (C7) and the force on the composite object (C12) is obscure.

[1] A. Einstein and L. Hopf, Statistische Untersuchung der Bewegung eines Resonators in einem Strahlungsfeld, *Ann. Phys. (Leipzig)* **338**, 1105 (1910).

[2] V. Mkrtchian, V. A. Parsegian, R. Podgornik, and W. M. Saslow, Universal thermal radiation drag on neutral objects, *Phys. Rev. Lett.* **91**, 220801 (2003).

[3] G. V. Dedkov and A. A. Kyasov, Tangential force and heating rate of a neutral relativistic particle mediated by equilibrium background radiation, *Nucl. Instrum. Methods Phys. Res., Sect. B* **268**, 599 (2010).

[4] G. Lach, M. DeKieviet, and U. D. Jentschura, Einstein-Hopf drag, Doppler shift of thermal radiation and blackbody drag: Three perspectives on quantum friction, *Cent. Eur. J. Phys.* **10**, 763 (2012).

[5] G. Pieplow and C. Henkel, Fully covariant radiation force on a polarizable particle, *New J. Phys.* **15**, 023027 (2013).

[6] A. I. Volokitin, Friction force at the motion of a small relativistic neutral particle with respect to blackbody radiation, *JETP Letters*, **101**, 427–433 (2015).

[7] A. I. Volokitin and B. N. J. Persson, *Electromagnetic Fluctuations at the Nanoscale* (Springer, Berlin, 2017).

[8] E. V. Teodorovich, Contribution of macroscopic van der Waals interactions to frictional force, *Proc. R. Soc. Lond. A* **362**, 71–77 (1978).

[9] L. S. Levitov, Van der Waals friction, *Europhys. Lett.* **8**, 499–504 (1989).

[10] J. B. Pendry, Shearing the vacuum—quantum friction, *J. Phys. Condens. Matter* **9**, 10301 (1997).

[11] A. I. Volokitin and B. N. J. Persson, Theory of friction: The contribution from a fluctuating electromagnetic field, *J. Phys. Condens. Matter* **11**, 345 (1999).

[12] G. V. Dedkov and A. A. Kyasov, The relativistic theory of fluctuation electromagnetic interactions of moving neutral particles with a flat surface, *Phys. Solid State* **45**, 1815 (2003).

[13] P. C. W. Davies, Quantum vacuum friction, *J. Opt. B* **7**, S40 (2005).

[14] G. Barton, On van der Waals friction. II: Between atom and half-space, *New J. Phys.* **12**, 113045 (2010).

[15] R. Zhao, A. Manjavacas, F. J. G. de Abajo, and J. B. Pendry, Rotational quantum friction, *Phys. Rev. Lett.* **109**, 123604 (2012).

[16] M. G. Silveirinha, Theory of quantum friction, *New J. Phys.* **16**, 063011 (2014).

[17] G. Pieplow and C. Henkel, Cherenkov friction on a neutral particle moving parallel to a dielectric, *J. Phys. Condens. Matter* **27**, 214001 (2015).

[18] F. Intravaia, V. E. Mkrtchian, S. Y. Buhmann, S. Scheel, D. A. R. Dalvit, and C. Henkel, Friction forces on atoms after acceleration, *J. Phys. Condens. Matter* **27**, 214020 (2015).

[19] J. S. Høye, I. Brevik and K. A. Milton, The reality of Casimir friction [arXiv:1508.00626], *Symmetry* **8** (5), 29 (2016), doi:10.3390/sym8050029.

[20] D. Pan, H. Xu, and F. J. García de Abajo, Magnetically activated rotational vacuum friction, *Phys. Rev. A* **99**, 062509 (2019).

[21] G. V. Dedkov and A. A. Kyasov, Nonlocal friction forces in the particle-plate and plate-plate configurations: Nonretarded approximation, *Surface Sci.* **700**, 121681 (2020).

[22] M. B. Farías, F. C. Lombardo, A. Soba, P. L. Villar, and R. Decca, Towards detecting traces of non-contact quantum friction in the corrections of the accumulated geometric phase, *npj Quantum Information* **6**, 25 (2020). <https://doi.org/10.1038/s41534-020-0252-x>

[23] G. V. Dedkov, Nonequilibrium Casimir-Lifshitz force and anomalous radiation heating of a small particle, arXiv:2207.13769.

[24] M. Oelschläger, Fluctuation-induced phenomena in nanophotonic systems, Ph.D. thesis, Institut für Physik, Humboldt Universität zu Berlin, 2020.

[25] T.-B. Wang, Y. Zhou, H.-Q. Mu, K. Shehzad, D.-J. Zhang, W.-X. Liu, T.-B. Yu, and Q.-H. Liao, Enhancement of lateral Casimir force on a rotating body near a hyperbolic material, *Nanotechnology* **33**, 245001 (2022).

[26] I. Brevik, B. Shapiro, and M. G. Silveirinha, Fluctuational electrodynamics in and out of equilibrium, *Int. J. Mod. Phys. A* **37**, 2241012 (2022).

[27] X. Guo, K. A. Milton, G. Kennedy, W. P. McNulty, N. Pourtolami, and Y. Li, Energetics of quantum vacuum friction: Field fluctuations, [arXiv:2108.01539] *Phys. Rev. D* **104**, 116006 (2021).

[28] X. Guo, K. A. Milton, G. Kennedy, W. P. McNulty, N. Pourtolami, and Y. Li, Energetics of quantum vacuum friction. II: Dipole fluctuations and field fluctuations, [arXiv:2204.10886], *Phys. Rev. D* **106**, 016008 (2022).

[29] D. Reiche, F. Intravaia, J.-T. Hsiang, K. Busch, and B.-L. Hu, Nonequilibrium thermodynamics of quantum friction, *Phys. Rev. A* **102**, 050203(R) (2020).

[30] M. Krüger, T. Emig, and M. Kardar, Nonequilibrium Electromagnetic Fluctuations: Heat transfer and interactions, *Phys. Rev. Lett.* **106**, 210404 (2011).

[31] A. Ott, P. Ben-Abdallah, and S.-A. Biehs, Circular heat and momentum flux radiated by magneto-optical nanoparticles, *Phys. Rev. B* **97**, 205414 (2018).

[32] M. F. Maghrebi, A. V. Gorshkov, and J. D. Sou, Fluctuation-induced torque on a topological insulator out of thermal equilibrium, *Phys. Rev. Lett.* **123**, 055901 (2019).

[33] C. Khandekar and Z. Jacob, Thermal spin photonics in the near-field of nonreciprocal media, *New J. Phys.* **21**, 103030 (2019).

[34] C. Khandekar, S. Buddhiraju, P. R. Wilkinson, J. K. Gimzewski, A. W. Rodriguez, C. Chase, S. Fan, Nonequilibrium lateral force and torque by thermally excited nonreciprocal surface electromagnetic waves, *Phys. Rev. B* **104**, 245433 (2021).

[35] H. C. Fogedby and A. Imparato, Autonomous quantum rotator, *EPL* **122**, 10006 (2018).

[36] C. Guo and S. Fan, Theoretical constraints on reciprocal and non-reciprocal many-body radiative heat transfer, [arXiv:2007.13274] *Phys. Rev. B* **102**, 085401 (2020).

[37] Y. Guo and S. Fan, A single gyroscopic particle as a heat engine, [arXiv:2007.11234] *ACS Photonics* **8**, 1623–1629 (2021).

[38] D. Gelbwaser-Klimovsky, N. Graham, M. Kardar, and M. Krüger, Near field propulsion forces from nonreciprocal media, *Phys. Rev. Lett.* **126**, 170401 (2021).

[39] B. Strekha, S. Molesky, P. Chao, M. Krüger, and A. Rodriguez, Trace expressions and associated limits for non-equilibrium Casimir torque, [arXiv:2207.13646] *Phys. Rev. A* **106**, 042222 (2022).

[40] L. Ge, Negative vacuum friction in terahertz gain systems, *Phys. Rev. B* **108**, 045406 (2023).

[41] V. S. Asadchy, M. S. Mirmoosa, A. Diaz-Rubio, S. Fan, and S. A. Tretyakov, Tutorial on electromagnetic nonreciprocity and its origins, *Proc. IEEE*, **108**, (10) 1684–1727 (2020) [arXiv:2001.04848].

[42] K. A. Milton, X. Guo, G. Kennedy, N. Pourtolami, and D. M. DelCol, Vacuum torque, propulsive forces, and anomalous tangential forces: Effects of nonreciprocal media out of thermal equilibrium, [arXiv:2306.02197] *Phys. Rev. A* **108**, 022809 (2023).

[43] G. Kennedy, Quantum torque on a non-reciprocal body out of thermal equilibrium and induced by a magnetic field of arbitrary strength, *Eur. Phys. J. Spec. Top.* **232**, 3197–3208 (2023). <https://doi.org/10.1140/epjs/s11734-023-01068-0>

[44] M. T. H. Reid, O. D. Miller, A. G. Polimeridis, A. W. Rodriguez, E. M. Tomlinson, and S. G. Johnson, Photon torpedoes and Rytov pinwheels: Integral-equation modeling of non-equilibrium fluctuation-induced forces and torques on nanoparticles, *arXiv:1708.01985* (2017).

[45] B. Müller and M. Krüger, Anisotropic particles near surfaces: Propulsion force and friction, *Phys. Rev. A* **93**, 032511 (2016).

[46] Quantum Vacuum Thruster, Scholarly Community Encyclopedia, <https://encyclopedia.pub/entry/28846>

[47] V. A. Parsegian, *Van der Waals Forces: A Handbook for Biologists, Chemists, Engineers, and Physicists* (Cambridge University Press, 2006), p. 268.

[48] H. Levine and J. Schwinger, On the theory of electromagnetic wave diffraction by an aperture in an infinite plane conducting screen, *Comm. Pure Appl. Math. III*, **4**, 355 (1950), reprinted in K. Milton and J. Schwinger, *Electromagnetic Radiation: Variational Methods, Waveguides, and Accelerators* (Springer, Berlin, 2006).